Idaho
National
Engineering
Laboratory

INEEL/EXT-97-01461
Distribution Category: UC-425

January 1998

Fusion Safety Program Annual Report Fiscal Year 1997

Glen R. Longhurst
Robert A. Anderl
Lee C. Cadwallader
W. Jon Carmack
J. Stephen Herring
Kathryn A. McCarthy
Brad J. Merrill
Richard L. Moore
David A. Petti
Steven T. Polkinghorne
Galen R. Smolik

LOCKHEED MARTIN

DISCLAIMER

INEEL/EXT-97-01461

Distribution Category: UC-425

Fusion Safety Program Annual Report Fiscal Year 1997

Glen R. Longhurst
Robert A. Anderl
Lee C. Cadwallader
W. Jon Carmack
J. Stephen Herring
Kathryn A. McCarthy
Brad J. Merrill
Richard L. Moore
David A. Petti
Steven T. Polkinghorne
Galen R. Smolik

Published January 1998

Idaho National Engineering and Environmental Laboratory
Nuclear Engineering Technologies Department
Lockheed Martin Idaho Technologies Company
Idaho Falls, Idaho 83415

Prepared for the
U.S. Department of Energy
Office of Energy Research
Under DOE Idaho Operations Office
Contract DE-AC07-94ID13223

DISCLAIMER

Portions of this document may be illegible electronic image products. Images are produced from the best available original document.

ABSTRACT

This report summarizes the major activities of the Fusion Safety Program in FY 1997. The Idaho National Engineering and Environmental Laboratory (INEEL) is the designated lead laboratory, and Lockheed Martin Idaho Technologies Company is the prime contractor for this program. The Fusion Safety Program was initiated in FY 1979 to perform research and develop data needed to ensure safety in fusion facilities. Activities include experiments, analysis, code development and application, and other forms of research. These activities are conducted at the INEEL, different DOE laboratories, and other institutions. The technical areas covered in this report include chemical reactions and activation product release, tritium safety, risk assessment failure rate database development, and safety code development and application to fusion safety issues. Most of this work has been done in support of the International Thermonuclear Experimental Reactor (ITER) project. Work done for ITER this year has focused on developing the needed information for the Non-site Specific Safety Report (NSSR-2).

CONTENTS

FIGURES

TABLES

ACRONYMS

BET	specific surface area measurement
BPP	basic performance phase
CAV	cavity package
CMD	count median diameter
CMFP	cumulative maximum flux plot
CPM	consolidated powder metallurgy
DDD	design description document
DIII-D	Doublet III-D
DOE	Department of Energy
EBR-II	Experimental Breeder Reactor II
EDA	Engineering Design Activity
EDF	engineering design file
EPP	extended performance phase
FAST	Fusion Aerosol Source Test
FDI	fuel dispersal interaction
FMEA	failure modes and effects analysis
FSP	Fusion Safety Program
FW	first wall
FY	fiscal year
GBR	generic bypass room
GSD	geometric standard deviation
HPME	high pressure melt ejection
HTO	tritiated water
IAEA	International Atomic Energy Agency
ICE	ingress of coolant event
IEA	International Energy Agency
INEEL	Idaho National Engineering and Environmental Laboratory
ISU	Idaho State University
ITER	International Thermonuclear Experimental Reactor
JCT	Joint Central Team
JET	Joint European Torus
LANL	Los Alamos National Laboratory
LOCA	loss of coolant accident
LOFA	loss of flow accident
LOVA	loss of vacuum accident
LPME	low pressure melt ejection
MLD	master logic diagram
MMD	mass median diameter
NCSU	North Carolina State University
NSSR-2	Non-site Specific Safety Report - 2
OB/LIM	outboard baffle/limiter

PCA	primary candidate alloy
PFC	plasma-facing component
PHTS	primary heat transport system
PS	plasma sprayed
R&D	research and development
SAA	safety analysis and assessment
SAE	safety and environment
SEM	scanning electron microscope
SIRENS	Surface Interaction Experiment at North Carolina State
SNL	Sandia National Laboratories
TD	theoretical density
TFTR	Tokamak Fusion Test Reactor
TPE	Tritium Plasma Experiment
UTIAS	University of Toronto Institute for Aerospace Studies
UW	University of Wisconsin
VAPOR	Volatilization of Activation Products Oxides Reactor
VDE	vertical displacement event
VV	vacuum vessel
VVPSS	vacuum vessel pressure suppression system

FUSION SAFETY PROGRAM ANNUAL REPORT FISCAL YEAR 1997

INTRODUCTION

Fusion power has the potential to be an important energy source while remaining inherently safe with attractive environmental features. For the full safety potential to be realized, safety must be a consideration in all aspects of design and development. In addition to incorporating design features that will enhance the safety potential of fusion systems, this requires identifying safety and environmental concerns and developing materials and technology required to implement resolutions to those concerns.

In 1979, the U.S. Department of Energy established the Fusion Safety Program (FSP) to support safety in fusion development. The Idaho National Engineering and Environmental Laboratory (INEEL) is the designated lead laboratory, and in 1994 Lockheed Martin Idaho Technologies Company became the prime contractor for this program. The program focus is to develop safety and environmental goals for fusion energy production, to identify potential safety and environmental concerns in fusion devices and approaches to resolve these concerns, and to develop technical information, risk assessment methodologies, and safety-analysis computer codes required to verify that fusion facilities are safe and environmentally attractive.

Realization of fusion's potential will result from advances in plasma physics and technology that will enhance safety, environmental, and economic attractiveness. Plasma physicists are addressing issues of plasma disruptions, runaway electrons, emergency plasma shutdown, control of power levels, and reduction of tritium throughput. Priorities in the technology area include developing plasma-facing components that are low in activation products and have minimal threats of chemical reactions that could produce explosive quantities of hydrogen. Ultimately, low activation materials will need to be developed for all components and structures exposed to fusion neutrons. Having appropriate and useful standards in place for the design of fusion facilities for safety is also of great importance. The FSP places a high emphasis on providing technical support and guidance in these critical areas.

International cooperation has become an increasingly important part of the FSP at the INEEL. In addition to participating with Japan, the European Union, and the Russian Federation in the International Thermonuclear Experimental Reactor (ITER) project, the FSP participates in activities of the International Energy Agency.

Activities performed during this fiscal year include conducting experimental tests to develop data needed for safety analyses, developing and applying computer codes and methodology for safety analyses, and

participating in studies that support safety in fusion development. Additionally, the FSP provided support to the ITER project by furnishing an individual to the ITER Joint Central Team and providing analysis and guidance in support of ITER safety studies. Another activity this year has been the preparation of a DOE Handbook, DOE HDBK 6004-97, Suppelementary Guidance and Design Experience for the Fusion Safety Standards DOE-STD-6002-96 and DOE-STD-6003-96. This handbook was written to capture information not included in the two DOE technical standards for safety of magnetic fusion facilities previously produced.

The following sections summarize work completed under each of these activities by the INEEL and participating organizations. Much of the work on ITER design studies and programmatic activities appears under the various technical areas in which the work was performed. Appendix A contains abstracts of publications based on work completed during FY 1997. Appendix B contains abstracts of engineering design files (EDFs) submitted to the ITER project. Most of the technical information developed by the Fusion Safety Program is in the EDF format.

INTERNATIONAL THERMONUCLEAR EXPERIMENTAL REACTOR DESIGN AND REGULATORY SUPPORT

Researchers: D. A. Petti, J. G. Crocker and S. J. Piet

The Fusion Safety Program (FSP) leads the U.S. safety and environmental (SAE) effort for the International Thermonuclear Experimental Reactor (ITER). ITER participants are the United States, the European Union, the Russian Federation, and Japan.

As part of the ITER effort, Dr. S. J. Piet was seconded to the ITER Joint Central Team (JCT). He served as Group Leader for Safety Analysis and Assessment (SAA). Dr. D. A. Petti is the Task Area Leader for Safety and Standards within the U.S. ITER Home Team.

Major Accomplishments

Dr. Piet and the SAA group are responsible for the overall technical and management integration of ITER accident safety. The group's major accomplishment this year has been the completion of the Non-site Specific Safety Report (NSSR-2)[1]. NSSR-2 is a comprehensive plant-level safety assessment that can be used by the participants to prepare the environmental paperwork required for site selection. NSSR-2 is a formal ITER milestone and another major step toward ITER regulatory approval and construction[2] and toward a safety approach appropriate for fusion energy.[3,4]

Piet coordinated the radioactivity confinement strategy. This strategy starts with equipment required for tokamak operation, including the vacuum vessel and cryostat vessel (see Figure 1). Heat transfer system vaults have been added to provide pressure containment for pressurized water coolant, as in a fission plant. The confinement performance of surrounding volumes and the tritium plant confinement are tailored (as in a chemical plant) to the specific hazard that resides in each volume.

NSSR-1 and NSSR-2 safety analyses of ITER reference accidents show that the confinement serves to meet the project dose

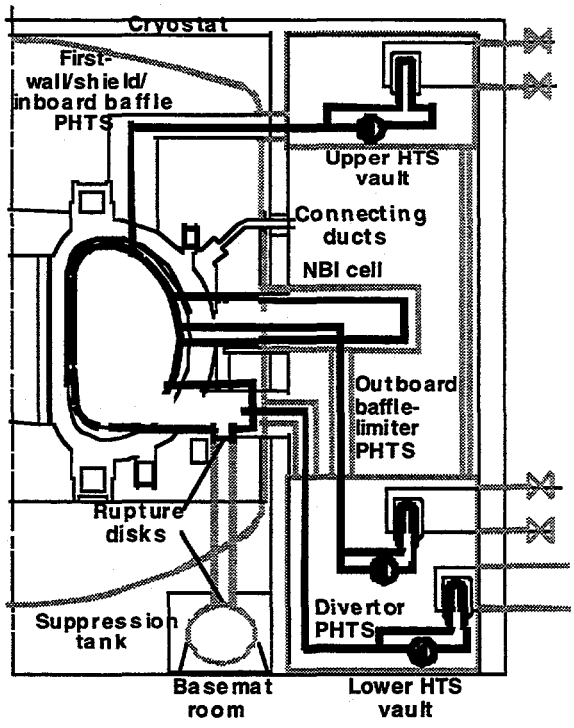

Figure 1. Tokamak elevation view showing ITER first and second confinement barriers; thick lines are first barrier, lighter gray lines are second barrier.

and release limits.[1,5-7] Table 1 shows the largest releases for seven different NSSR-2 reference accidents. In all other reference accidents, releases are below 0.1% of the project limit.

Table 1. ITER NSSR-2 events with largest radiological releases expressed as percent of project limit

Event No.	Category II Events	Percent of Limit
2.3	Heat Exchanger leak	6.70%
2.6	Air leakage in vacuum vessel during maintenance	2.05%
	Category III Events	**Percent of Limit**
3.3	Vacuum Vessel pipe break	1.91%
3.5	Heat Exchanger tube rupture	2.96%
	Category IV Events	**Percent of Limit**
4.4	Wet bypass	28.20%
4.6	Loss of vacuum	19.72%
4.7	Stuck Divertor cassette	10.01%

Piet also coordinated the ITER "source term," integrating information from several of the home team tasks, most notably the U.S. Fusion Safety Program. This effort is steadily resolving uncertainties.[8] Additional information on source term research and development (R&D) results are found in later sections of this report.

The goal of the ITER design and regulatory support work in the Fusion Safety Program is to provide ITER safety and regulatory support to the JCT and to improve the safety of ITER by identifying key safety issues associated with the evolving ITER Engineering Design Activities (EDA). Furthermore, the group works with the ITER Joint Central Team and safety colleagues in the other home teams to ensure the safety and environmental attractiveness of ITER and to demonstrate that it can be sited in any of the sponsoring Parties with a minimum of site-specific redesign. Efforts have been focused on developing an international consensus approach for ITER safety design and assessment, including development of general safety and environmental design criteria, quantitative dose-release assessment criteria, and a radiation protection program; waste characterization; and development of safety analysis guidelines.[9]

The high level of interaction, cooperation, and collaboration between the Joint Central Team and the home teams and between the safety team and designers, and the spirit of consensus that has guided them, have resulted in a safe design for ITER and a safety assessment that can meet the needs of the potential host countries.

Much of the safety design work this year was in support of NSSR-2 accident analyses and risk studies. These topics are discussed later in the appropriate technical sections of this report.

In addition to providing regulatory information for the ITER JCT, the U.S. ITER task area leader for safety and standards also made a number of presentations on ITER safety and regulatory issues to U.S. groups such as the Fusion Energy Sciences Advisory Committee.[10]

Future Activities

Future efforts will continue work with the JCT on their regulatory and safety strategy for ITER and help them complete future safety documents as the ITER EDA ends and the project moves into the transition phase prior to ITER construction.

References

1. *Non-Site Specific Safety Analysis Report (NSSR-2)*, ITER Joint Central Team, San Diego, CA December 1997.

2. Y. Shimomura, et al, "ITER Safety Issues," *IAEA Fusion Conference, Montreal, October 6-12, 1996.*

3. D. A. Petti and S. J. Piet, "An Overview of ITER Safety," *Fusion Technology*, Vol. ***30,*** Part 2A, December 1996, pp. 586-593.

4. A. E. Poucet and S. J. Piet, "Safety Analysis and Design Framework in ITER," *ANS-PSA 96 Probabilistic Safety Assessment: Moving toward Risk Based Regulation, Park City, Utah, September 29 - October 3, 1996.*

5. H.-W. Bartels, et al., "Fusion Specific Features in ITER Accident Analysis," *Journal of Fusion Energy*, Vol. ***60,*** No. 1/2, 1997, pp. 3-10.

6. W. Gulden, et al., "Analysis of ITER Accident Sequences," *Proceedings of the 19th Symposium on Fusion Technology (SOFT), Lisbon, Portugal, September 16-20 1996*, pp. 1755-1758.

7. S. J. Piet, et al., "ITER Inherent/Passive Ultimate Safety Margins," *International Symposium on Fusion Nuclear Technology-4, Tokyo, Japan, April 1997.*

8. S. J. Piet, et al., "Source Term and Mobilization Assessment in NSSR-1," *Journal of Fusion Energy*, Vol. ***60,*** No. 1/2, 1997, pp. 11-18.

9. C. Gordon, et al., "International Cooperation in the Safety and Environmental Assessment for the ITER Engineering Design Activities," to be presented at the 11th Pacific Basin Nuclear Conference, Banff, Canada, May 1998.

10. D. A. Petti, "An Overview of ITER Safety," Presentation to U.S. Fusion Energy Sciences Advisory Committee, San Diego, CA, January 1997.

ACTIVATION PRODUCT MOBILIZATION AND TRANSPORT

Researchers: K. A. McCarthy, G. R. Smolik, W. J. Carmack, K. Coates, and D. A. Petti—INEEL, J. P. Sharpe, M. Bourham, and J. G. Gilligan—NCSU, S. Gorman—ISU

Fusion neutrons generated during the deuterium-tritium reaction will produce activation products. Since activation products are an accident concern, INEEL researchers are examining their behavior under accident conditions, working to characterize the oxidation-driven mobilization and plasma-disruption-generated activation product source terms. This task focuses on materials for the divertor, first wall, blanket, and shield, and their behavior at accident temperatures in air and steam oxidizing environments.

Major Accomplishments

The main focus this year was on characterization of tokamak dust. A protocol was developed for collecting dust from existing tokamaks, and constructing size distributions. Dust collected from DIII-D at General Atomics, located in La Jolla, California, and Alcator C-MOD, at the Massachusetts Institute of Technology, located in Cambridge, Massachusetts was analyzed as was dust produced in the SIRENS plasma gun disruption simulator at North Carolina State University. In addition to the dust work, development continued on the database for oxidation-driven mobilization. The team completed a series of tests to measure stainless steel mobilization in air in the FAST facility and validated previously gathered stainless steel data, including compiling data from the FAST and VAPOR experimental facilities.

Characterization of Dust from Operating Tokamaks. Tokamak dust, accumulated primarily from sputtering and disruptions, has important safety issues associated with it.[1] The dust may contain tritium; and it may be activated, chemically toxic, and chemically reactive. The size of the dust and the surface area are important parameters in determining potential hydrogen production and transport of activated/chemically toxic dust. A protocol was developed for dust collection with the goal of preserving the particle size distribution and physical characteristics of the dust. Choice of collection technique is important because the sampling technique used can bias the particle size distribution collected.[2-4]

Particulate was collected from the DIII-D tokamak, a machine with carbon as the primary plasma-facing material. Two methods were used to collect particulate from the tokamak: vacuum collection on substrates and adhesion removal with metallurgical replicating tape.[2-5] The multi-step procedure used to construct a particle size distribution from substrate data obtained with the optical microscope and has been developed specifically for this research. The flowchart in Figure 2 describes the procedure.

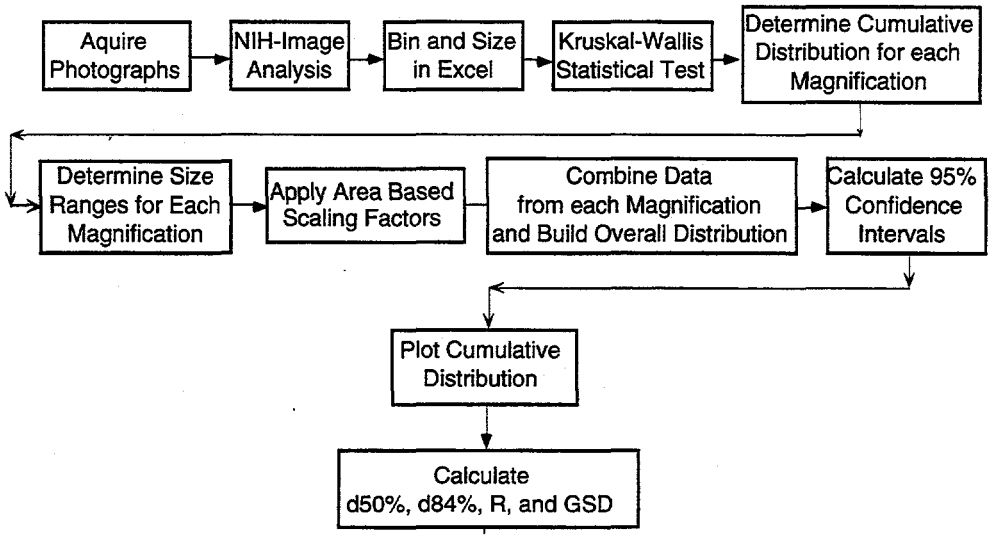

Figure 2. Flow chart schematic of particle size distribution construction.

The optical microscope method is capable of counting particles with diameters in the range of 0.15 μm to 300 μm. Particles larger than 300 μm begin to exceed the viewable area of the microscope and particles smaller than 0.15 μm are not resolvable because they are too small to be seen within the magnification capability of the microscope.

Figure 3 shows the particle size distribution results for Quadrant 1 of the tokamak (dust was collected in each of four regions, or quadrants) for the "gross" vacuum (the general area located within the quadrant of interest) and "detail" vacuum (four specific tiles of interest). Also shown in the figure are the ranges selected for inclusion in the overall cumulative probability distribution.

The count median diameters (the particle size for which half the total number of particles are larger and half smaller) for particles collected in various locations in the DIII-D tokamak did not vary greatly, ranging from 0.5 μm to 0.86 μm with geometric standard deviations ranging from 2.0 to 3.5.

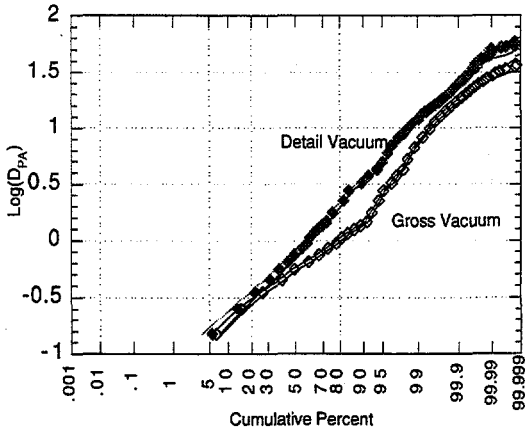

	Detail Vacuum	Gross Vacuum	Area Scaling Factor
100 X	0 - 1.0 μm	0 - 1.0 μm	400
50 X	1.0 - 1.5 μm	1.0 - 1.5 μm	100
20 X	Not Used	Not Used	16
10 X	1.5 - 4.5 μm	1.5 - 4.5 μm	4
5 X	4.5 μm and up	4.5 μm and up	1
$d_{50\%}$ (μm)	0.503	0.706	
$d_{84\%}$ (μm)	1.55	1.85	
GSD	3.08	2.62	
R	0.9906	0.9983	

Figure 3. Overall cumulative probability distribution for Quadrant 1 detail and gross vacuums from DIII-D.

Dust collected from the Alcator C-MOD tokamak was also analyzed.[6] This tokamak has molybdenum plasma facing surfaces. The sample obtained from C-MOD was not originally intended for outside examination, however C-MOD personnel made some available for analysis. This dust was meant to be used only for chemical analysis, thus during collection, care was not taken to collect a sample with a size distribution representative of the size distribution of the dust in the tokamak. The filter used in the vacuum collection had a pore size of 2 μm, which may have resulted in the loss of smaller particulate.

The count median diameters of the samples analyzed ranged from 0.61 μm to 1.1 μm with geometric standard deviations ranging from 2.8 to 5.2. Figure 4 shows the cumulative log probability distribution generated for one of the C-MOD samples.

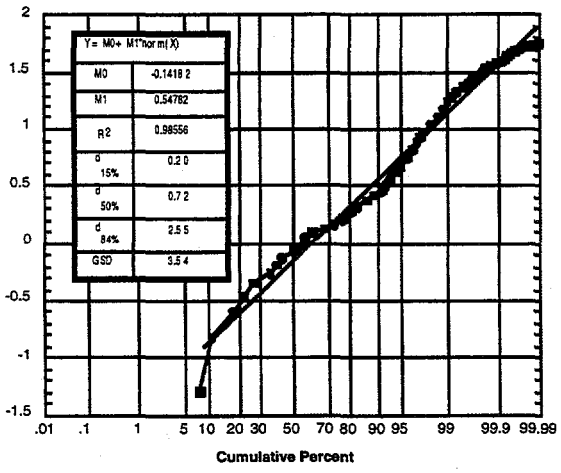

Figure 4. Overall cumulative log probability distribution for a sample collected from Alcator C-MOD.

Aerosol Mobilization from Disruptions. The purpose of this task is to characterize and quantify the material mobilized during a disruption. The SIRENS electro-thermal plasma gun at North Carolina State University is being used to perform these studies. The same sizing protocol developed for analysis of tokamak dust[2] was used to calculate particle size distributions for the particulate produced by the SIRENS plasma gun. Prior to experiments to produce data for safety analyses, a series of scoping tests was carried out to ensure that the correct experimental parameters can be attained and adequate quality control procedures are in place.[7-8]

After completion of the scoping tests, a series of tests was completed with copper, stainless steel, tungsten, and aluminum (to simulate beryllium).[9] Particulate collected and analyzed from the various metals displayed count median diameters from 0.3 to 3.0 μm. The particle sizes appeared independent of the material tested. The minimum and maximum observed particle sizes were 0.075 μm and 50 μm, respectively. The majority of the particles in the underlying distributions, however, were approximately 1 μm. Figure 5 shows the cumulative log probability distribution for Button 7 (near the end of the expansion chamber) of one of two tungsten tests.

Oxidation-Driven Mobilization Task. Work concentrated this year on stainless steel mobilization. Four tests were completed in the FAST facility, one each at 500, 600, 700, and 800°C.[10] These data, along with data from earlier tests in FAST with a steam environment, were compared with data obtained in the smaller-scale VAPOR facility.[11-12] Through committee review, data was selected to be used for

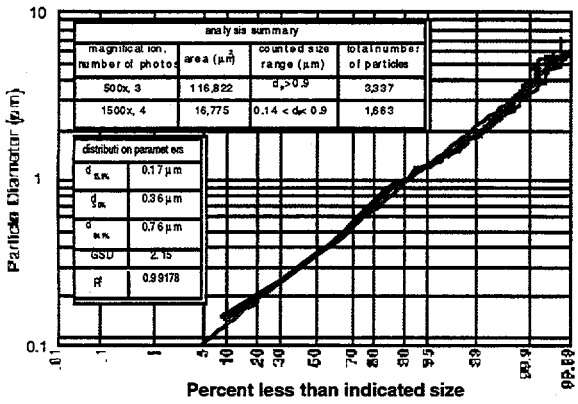

Figure 5. Cumulative log probability distribution for Button 7 of a tungsten test in the SIRENS plasma gun facility.

constructing cumulative maximum flux plots (CMFPs) for various elements for exposures in air and steam. These values are recommend for safety studies involving accidents with ingress of air or steam.

From a mechanistic standpoint, the research found that particles of spalled oxide are responsible for most (generally greater than 90%) of the mobilization from austenitic stainless steels for steam exposures. Longer tests in VAPOR produced thicker oxides, which combined with the sharp corners on the VAPOR specimens, resulted in more spalled oxide being collected in VAPOR. Less spalled oxide was generated in FAST due to shorter oxidation times and the absence of sharp corners. Molybdenum and chromium show strong evidence of mobilization by volatilization processes during air exposures.

The plots use FAST data at lower temperatures where better detection limits are obtained and VAPOR data at higher temperatures where higher contributions from spalled oxide provide measures of conservatism in mobilization rates for the CMFPs.

Future Activities

Work will continue to analyze dust collected from operating tokamaks, including TFTR at the Princeton Plasma Physics Laboratory and an additional collection and analysis of dust from Alcator C-MOD at MIT. Characterization of plasma-disruption induced aerosols will continue, concentrating on carbon and mixed materials. A first-principles modeling effort to support these experiments will begin . Mobilization of plasma-sprayed beryllium in air and steam will be measured in VAPOR. The data validation effort will continue, concentrating in the upcoming year on tungsten mobilization data.

References

1. K. A. McCarthy, D. A. Petti, W. J. Carmack, and G. R. Smolik, "The Safety Implications of Tokamak Dust Size and Surface Area," presented at the *Fourth International Symposium on Fusion Nuclear Technology, Tokyo, Japan, April 7-11, 1997*, to be published in *Fusion Engineering and Design.*

2. W. J. Carmack, M. E. Engelhardt, and P. B. Hembree, *DIII-D Dust Particulate Characterization*, Engineering Ddesing File ITER/US/97/TE/SA-8, March, 1997.

3. W. J. Carmack, K. A. McCarthy, D. A. Petti, A. G. Kellman, and C. P-C. Wong, "Collection and Analysis of Particulate from the DIII-D Tokamak," presented at the *Fourth International Symposium on Fusion Nuclear Technology, Tokyo, Japan, April 7-11.*

4. W. J. Carmack, M. E. Engelhardt, P. B. Hembree, Kathryn A. McCarthy, and David A. Petti, *DIII-D Dust Particulate Characterization*, INEEL/EXT-97-00702, November, 1997.

5. W. J. Carmack and P. B. Hembree, *Revision of DIII-D Quadrant 2 Detail Vacuum Analysis*, Engineering Design File ITER/US/97/TE/SA-16, July, 1997.

6. S. V. Gorman, W. J. Carmack, and P. B. Hembree, *C-MOD Particulate Characterization*, Engineering Design File ITER/US/97/TE/SA-17, August, 1997.

7. J. P. Sharpe, M. Bourham, and J.G. Gilligan, "Experimental Investigation of Disruption-Induced Aerosol Mobilization in Accident Scenarios of ITER," presented at the *17th IEEE/NPSS Symposium on Fusion Engineering, San Diego, California, October 6-9, 1997.*

8. J. P. Sharpe and M. Bourham, *Scoping of SIRENS for Wall Material Vaporization Studies*, Engineering Design File ITER/US/97/TE/SA-14, June, 1997.

9. J. P. Sharpe, *Characterization of Disruption-Induced Particulate from ITER Relevant Metals*, Engineering Design File ITER/US/97/TE/SA-21, November, 1997.

10. W. J. Carmack, *Fusion Aerosol Source Test (FAST) Air Exposure of 316SS*, Engineering Design File ITER/US/97/TE/SA-15, May 31, 1997.

11. G.R. Smolik, K.A. McCarthy, W.J. Carmack, and K. Coates, "Mobilization from Austenitic Stainless Steel in Air and Steam: Recent Tests, Compilation of Data from Tests to Date, and Resulting Dose Calculations," presented at the *17th IEEE/NPSS Symposium on Fusion Engineering, October 6-9, 1997, San Diego, California.*

12. G. R. Smolik, W. J, Carmack, and K. Coates, *Mobilization from Austenitic Stainless Steels During Air and Steam Exposures*, Engineering Design File ITER/US/97/TE/SA-25, December 1997.

CHEMICAL REACTIVITY

Researchers: K. A. McCarthy, R. A. Anderl, M. A. Oates, R. J. Pawelko, G. R. Smolik—INEEL

Evaluation of the safety hazards for fusion reactors includes an assessment of the failures of plasma facing component materials due to various accident scenarios. One scenario is a loss of coolant accident (LOCA) in which a water-line break injects steam into the torus vacuum vessel. The hot plasma-facing material can react with the steam, producing hydrogen. In this task the chemical reactivity of plasma facing materials is studied.

Major Accomplishments

The primary focus this year was to measure the chemical reactivity (specifically, the hydrogen production) of plasma-sprayed (PS) beryllium and irradiated beryllium exposed to steam. In addition, the chemical reactivity of Russian TGP-56 beryllium was measured to compare the behavior of the Russian beryllium relative to U.S. beryllium tested here over the past several years.

Chemical Reactivity of Plasma-Sprayed Beryllium. Test specimens for this work were fabricated at the Beryllium Atomization and Thermal Spray Facility, Los Alamos National Laboratory (LANL). There were two different densities, 94% and 92% of theoretical density (TD). The approach in this work was to characterize the density, porosity and specific surface area for the specimens and to measure the chemical reactivity of the specimens exposed to steam at various temperatures.[1]

Density and porosity characterization was based on liquid immersion density measurements, and BET specific surface areas were measured using a gas-adsorption technique with Kr as the adsorptive gas.[2] The immersion-density measurements gave bulk densities of 94%TD, with an open porosity of 1.4% and a closed porosity of 4.2%, and 92%TD, with 7.7% for open porosity and a statistically insignificant closed porosity. BET measurements and analyses gave specific surface areas of 0.085 m^2/g for the 94%TD PS material and 1.21 m^2/g and 1.07 m^2/g for two different specimens of 92%TD PS material. These porosity and surface-area results were compared to corresponding results for Battelle plasma-sprayed Be tested in 1992 and for consolidated powder metallurgy (CPM) Be of varying density. For comparable bulk densities and porosity, the plasma-sprayed Be with bulk densities of 92%TD or less had much higher specific surface areas than CPM Be, reflecting a higher surface-area microstructure, i.e., flat splat-like features for PS Be compared to more round-shaped particles for CPM Be.

Chemical reactivity experiments were performed for the LANL PS-Be specimens exposed to steam at temperatures ranging from 350°C to above 1000°C. Hydrogen generation rates and parabolic rate constants were derived from mass-spectrometer measurements and from measurements of specimen weight-gain. These experiments

showed a complex Be-steam reactivity behavior, dependent primarily on the test temperature and the specimen open porosity and surface area. For temperatures of 450°C and less, the kinetics were parabolic. At 500°C, the reactivity was initially parabolic and subsequently became moderately accelerating as the steam exposure continued. For a temperature of 600°C, the 94%TD PS material exhibited an accelerating behavior and the 92%TD PS material showed a runaway behavior characterized by a large temperature excursion. For temperatures of 700°C and above, the 94%TD PS material showed both accelerating and linear behavior.

Results from the chemical-reactivity experiments for the LANL PS Be material were compared to corresponding results for Battelle PS Be and for fully-dense and porous CPM Be. At temperatures from 700°C and below, H_2 generation rates for the LANL 94%TD PS Be were about a factor of 100 higher than those for fully-dense CPM Be, however, the rates were significantly lower than those for LANL 92%TD PS Be, Battelle PS Be and porous CPM Be. Differences in the H_2 generation rates could be accounted for by the measured differences in surface area for the various materials. Figure 6 shows the results of the recent plasma-sprayed Be tests in comparison with earlier tests.

Chemical Reactivity of Irradiated Beryllium. This series of experiments was a follow-on to a series of experiments completed in 1996.[3] The beryllium samples were fully dense samples fabricated with powder metallurgy techniques. Irradiation of the 0.635-cm and 2.032-cm long beryllium samples took place in EBR-II as part of the

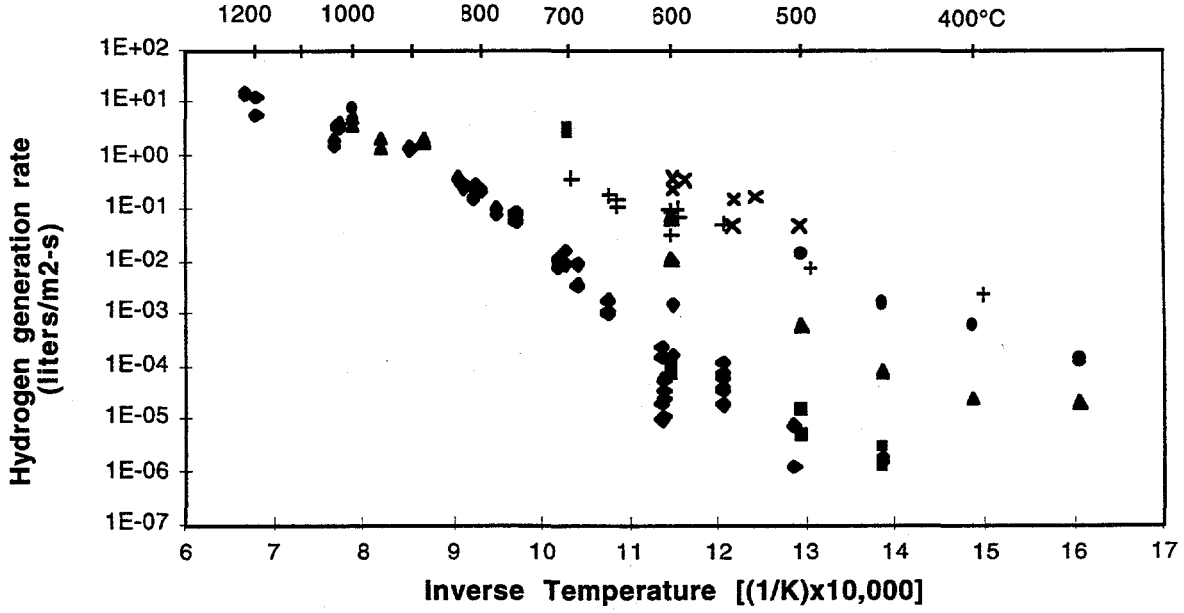

Figure 6. Recent plasma-spray beryllium test results (circles indicate 92%TD Be, triangles indicate 94%TD Be) are shown in comparison with previous data: 1992 plasma-sprayed Be (x's), porous Be tests (plus signs), 1996 irradiated Be tests (squares) and various shapes and sizes of fully dense CPM Be (diamonds).

COBRA-1A2 test.[4] Fast neutron fluences (>0.11 MeV) were estimated to range from 5.2×10^{22} n/cm^2 to 6.7×10^{22}n/cm^2 (more than an order of magnitude higher than the expected ITER first wall fluence). The nominal irradiation temperature was 400°C.

The purpose of the work was to determine the influence of neutron irradiation effects and annealing on the chemical reactivity of beryllium exposed to steam. The work entailed measurements of the H_2 generation rates for unirradiated and irradiated Be and for irradiated Be that had been previously annealed at different temperatures ranging from 450 to 1200°C.[5-6] The emphasis of this work was to relate chemical-reactivity data for irradiated Be to changes in the material porosity and surface area that result from heating.

Hydrogen generation rates were similar for irradiated and unirradiated Be in steam-chemical reactivity experiments at temperatures between 450 and 600°C. For irradiated Be exposed to steam at 700°C, the chemical reactivity accelerated rapidly and the specimen experienced a temperature excursion. Enhanced chemical reactivity at temperatures between 400 and 600°C was observed for irradiated Be annealed at temperatures of 700°C and higher. This reactivity enhancement could be accounted for by the increased specific surface area resulting from development of a surface-connected porosity in the irradiated-annealed Be. Figure 7 shows the results of this series of irradiated beryllium tests.

Chemical Reactivity of Russian Beryllium. Hydrogen generation rates were measured for Russian TGP-56 grade Be cylindrical specimens exposed to steam.[7] These fully-dense specimens were tested at 500, 600, 700, and 800°C, temperatures that provided a means to compare the observed chemical reactivities with those observed in previous tests for cylindrical Be control specimens. A comparison of the hydrogen

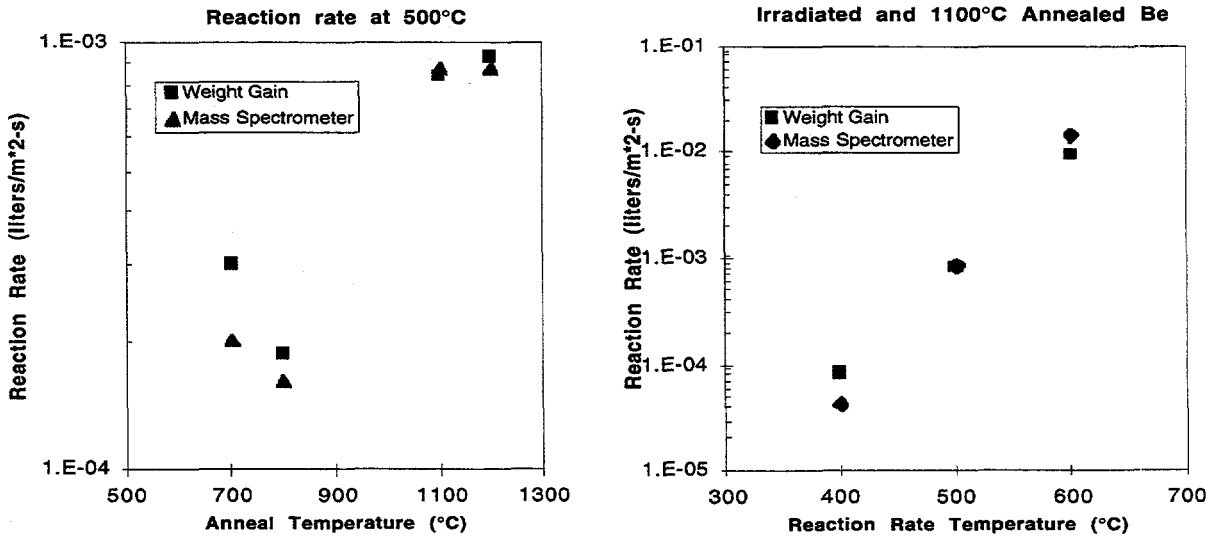

Figure 7. The reaction rate for beryllium, previously annealed at temperatures of 600-1100°C, tested in steam at 500°C, varies almost an order of magnitude due to the increased surface area introduced by the annealing process (figure on left). The figure on the right shows the reaction rate for irradiated beryllium annealed at 1100°C, then exposed to steam at temperatures of 400-600°C.

generation results indicates that both kinetic hydrogen generation rate behavior and average hydrogen generation rates are in reasonable agreement for the two types of specimens, especially for temperatures above 600°C. Differences in the hydrogen generation behavior for the two types of specimens at 600°C and below are attributed to possible differences in surface condition, an effect observed in multiple tests with the Be control specimens.

Effect of Surface Area on Chemical Reactivity of Beryllium. The capability to measure effective surface area has provided some unique insights into the effect of surface area on the chemical reactivity of beryllium. When the beryllium chemical reactivity data are plotted with respect to BET surface area (liters of hydrogen produced per square meter BET surface area, per second) rather than with respect to the geometrical surface area of the specimen, the plot in Figure 8 is the result. The spread in the data in Figure 8 is significantly less than the spread in the data in Figure 6. The difference in chemical reactivity between the various types of beryllium can be partially explained by the surface area available to react with the steam. Specimens with significant surface-connected porosity have more surface area available to react with the steam. More research is needed to better understand the chemical reactivity of various forms of beryllium.

Future Activities

An important upcoming activity is to begin development of a first-principles model to describe the chemical reactivity of various forms of beryllium. Planned experiments include measuring the chemical reactivity of plasma-sprayed beryllium in air and tests on tokamak dust chemical reactivity if a large enough sample of dust can be acquired. If irradiated beryllium samples with fluences characteristic of the ITER first wall can be obtained, those samples will also be tested.

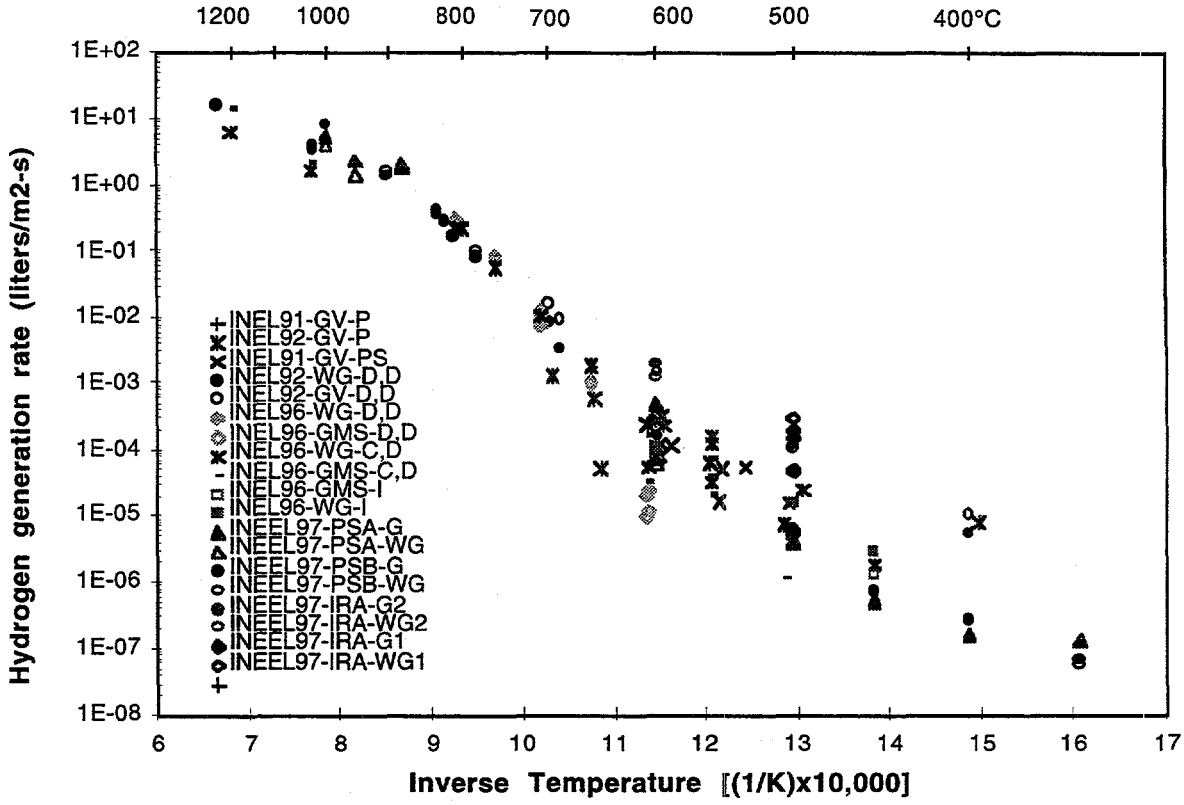

Figure 8. The difference in chemical reactivity of various forms of beryllium can be partially explained by effective surface area; plotting the hydrogen generation rate in terms of BET surface area can decrease the spread in the data significantly. Methods to determine hydrogen produced were gas collection (GV), weight gain (WG), mass spectrometer (GMS, G1, G2). Forms of beryllium shown are porous—88% dense (P), plasma-sprayed (PS, PSA, PSB), fully-dense discs (D), fully-dense cylinders (C), and irradiated fully dense (I, IRA).

References

1. R. A. Anderl, "Steam Reactivity Experiments for LANL Plasma-Sprayed Beryllium," Engineering Design File ITER/US/97/TE/SA-23, September 29, 1997.

2. G. R. Smolik, R. A. Anderl, R. J. Pawelko, W. J. Carmack, P. B. Hembree and M. A. Oates, "BET Surface Area Measurements of Materials for Fusion Safety Studies," presented at the *17th IEEE/NPSS Symposium on Fusion Engineering, San Diego, California, October 6-9, 1997.*

3. R. A. Anderl, R. J. Pawelko, M. A. Oates, G. R. Smolik, and K. A. McCarthy, "Steam-Chemical Reactivity Studies for Irradiated Beryllium," *Journal of Fusion Energy*, Vol. 16, 1996, pp. 1435-1441.

4. A. M. Ermi, *Preliminary Report on the Irradiation Parameters for the EBR-II COBRA-1A2 Test*, Westinghouse Hanford Company, November, 1994.

5. R. A. Anderl, K. A. McCarthy, M. A. Oates, D. A Petti, R. J. Pawelko, and G. R. Smolik, "Steam Chemical Reactivity for Irradiated Beryllium," presented at the *Third IAEA International Workshop on Beryllium Technology for Fusion, Sangyou Kaikan, Mito City, Japan, October 22-24, 1997.*

6. R. A. Anderl, K. A. McCarthy, M. A. Oates, D. A Petti, R. J. Pawelko, and G. R. Smolik, "Steam Chemical Reactivity for Irradiated Beryllium," presented at the *8th International Conference on Fusion Reactor Materials, Sendai, Japan, October 26-31, 1997.*

7. R. A. Anderl, *Steam-Chemical Reactivity Experiments for Russian TGP-56 Be*, Engineering Design File ITER/US/97/TE/SA-5, February 27, 1997.

TRITIUM SAFETY

Researchers: G. R. Longhurst, R. A. Anderl, M. A. Oates, and R. J. Pawelko—INEEL

The tritium safety work is focused on the International Thermonuclear Experimental Reactor (ITER) goals of keeping routine and accidental tritium releases within acceptable limits, thus avoiding the need for evacuation of the surrounding population. Work is pursuing a broad spectrum of tritium-related studies, including continued development of the Idaho National Engineering and Environmental Laboratory tritium laboratory capabilities; plasma-driven permeation studies involving plasma-facing materials; applications of the TMAP4 code, particularly with regard to tritium inventories in ITER; and assisting in the interpretation of experimental data from the Tritium Plasma Experiment (TPE) and other experiments.

Major Accomplishments

Studies of Deuterium Implantation/ Permeation. The facilities at the INEEL Tritium Research Laboratory were used to investigate effects on deuterium retention and release characteristics of carbon coatings on beryllium and tungsten. Samples consisting of 130-nm thick carbon coating on PF-60 beryllium were annealed in a resistance furnace for 2 hours at constant temperatures of 25, 300, 400, and 500°C. Depth-profile Auger analysis was then performed to study the elemental distribution in the surface layers. This analysis showed that for the 25 and 300°C tests, there was no appreciable movement of any of the materials. In the 400°C test, the carbon and beryllium had begun to intermix at the interface, and in the 500°C test, the mixing was complete with the C:Be ratio about 0.78 (43% C and 57% Be). These layers are believed to alter the tritium retention and release characteristics.

Interpretation of Experimental Data. Experiments conducted at various facilities to measure the amount of deuterium retained in beryllium surfaces subjected to deuterium implantation followed by thermal desorption were found to be correlated if the retained deuterium amounts were scaled for their various implantation depths due to differences in incident ion beam energy. This is demonstrated in Figure 9.

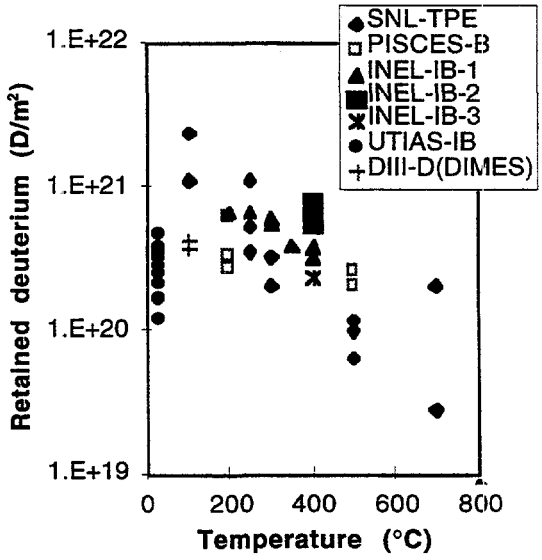

Figure 9. Correlation using implantation depth for deuterium retention in experiments at SNL,[1] PISCES-B,[2] INEEL,[3] UTIAS,[4] and JET.[5]

Specific support was provided to the ITER Design Co-Center in Garching in the area of tritium inventories in plasma-facing components. This is a significant safety issue as well as a design and operating issue.

Another significant accomplishment during the year was the development of a mechanistic model that successfully predicted the saturation effect observed in beryllium.[6] In this effect, hydrogen isotope atoms are deposited by ITER-like plasmas at such a high rate that surface-connected open porosity develops in the vicinity of the implantation zone. This has the effect of suppressing the driving potential for diffusion into the bulk of the material by rapidly recycling implanted atoms to the plasma. The result is a highly favorable reduction in tritium inventory and permeation rate.

Tritium Source Term Analysis. The models developed for tritium inventory and permeation estimates for the ITER basic performance phase (BPP)[6,7] were used to prepare estimates for the retention and permeation of tritium in the revised first wall and blanket structure of the extended performance phase (EPP).[8] Perhaps not surprisingly, the dominant inventory fraction (353 of 432 g total inventory at the end of the EPP) was tritium bred in the neutron multiplier blocks of the tritium breeding blanket. Of the tritium bred, more than a third was estimated to be released to the helium sweep gas stream.

Tritium Transport in Neutron Irradiated Beryllium. Incident to the analysis of tritium in the neutron multiplier blocks of the ITER breeding blanket, it was necessary to use estimates of tritium transport properties for less than fully dense neutron irradiated beryllium. Using the TMAP4 code, the experimental data of Baldwin and Billone[9] were analyzed for thermal desorption release of tritium from dense and less than fully dense beryllium that had been irradiated in a fission reactor. It was found that transport could be very adequately modeled using well accepted values of hydrogen diffusivity and solubility together with derived trapping characteristics of 0.3% atom fraction traps at 1.06 eV for the 81% dense beryllium tested and 2% atom fraction traps at 1.4 eV for the fully dense beryllium tested.[10]

Future Activities

Work will continue to focus on providing support for the Safety and Environmental Tasks of the ITER project, but broader issues will also be addressed. A specific objective will be to complete implantation/release experiments on samples of tungsten and beryllium coated with carbon that were delayed by a systematic error in thermal desorption inventory measurements discovered midway through the year. Work will also pursue by experiment and analysis the understanding of an apparent saturation effect in tungsten, similar to the one observed in beryllium. Another goal is the characterization of beryllium pebbles being considered for use in the ITER breeding blanket with respect to their hydrogen retention and release characteristics. User support will continue to be provided for the TMAP4 code that code will continue to be used in support of safety analyses for ITER and in other applicatons.

References

1. R. A. Causey, G. R. Longhurst, W. A. Harbin, "Tritium retention in S-65 beryllium after 100-eV plasma exposure," Journal of Nuclear Materials, Vol. 241-243, 1997, pp. 1041-1056.

2. R. Doerner et al., "Beryllium Plasma Interaction Measurements in PISCES-B," submitted to *Journal of Nuclear Materials.*

3. R. A. Anderl et al., "Deuterium Transport and trapping in polycrystalline tungsten," *Journal of Nuclear Materials,* Vol. 196-198, 1992, p. 745.

4. A. A. Haasz and J. W. Davis, "Deuterium retention in beryllium, molybdenum, and tungsten at high fluences," *Journal of Nucear Materials,* Vol. 241-243, 1997, p. 1076.

5. G. Saibene et al., "Hydrogen recycling coefficient in beryllium: Experimental determination and a test simulation of the density evolution in a JET plasma discharge," *Journal of Nuclear Materials,* Vol. 176&177, 1990, p. 618.

6. G. R. Longhurst, "Modeling of Hydrogen Plasma Interactions with Beryllium Surfaces," Engineering Design File ITER/US/97/TE/SA-1, January 10, 1997.

7. G. R. Longhurst, "Accounting for Tritium Breeding in Beryllium in TMAP4 Calculations," ITER/US/95/TE/SA-7, February 25, 1997.

8. G. R. Longhurst, "Tritium Inventories and Permeation Rates For The ITER Breeding Blanket And Metal-Coated Plasma-Facing Components In The Extended Performance Phase," Engineering Design File ITER/US/97/TE/SA-22 Rev. 1, September 24, 1997.

9. D. L. Balwin and M. C. Billone, "Diffusion/desorption of tritium from irradiated beryllium," *Journal of Nuclear Materials,* Vol. 212-215, 1994, pp. 948-953.

10. G. R. Longhurst, "Modeling of hydrogen interactions with beryllium," *3rd IEA International Workshop on Beryllium Technology for Fusion, Mito, Japan, October 22-24, 1998,* proceedings to appear.

RISK ASSESSMENT

Researchers: L. C. Cadwallader—INEEL, T. D. Marshall—Rensselaer Polytechnic Institute

The Fusion Safety Program (FSP) leads the U.S. effort in using risk assessment in fusion experiment design to provide safety for the public, workers, and the environment. Risk assessment is a part of the safety design effort for the International Thermonuclear Experimental Reactor (ITER). Two important features of fusion risk assessment are system analysis and radiological dose assessment. FY 1997 progress in the system analysis facet of fusion risk assessment work is discussed below.

Major Accomplishments

System Analysis. INEEL researchers supported work on the second version of the Non-site Specific Safety Report (NSSR-2). Research focused on developing a master logic diagram (MLD)[1] and on performing failure modes and effects analyses (FMEAs) for the cryogenic production plant and distribution system for ITER.[2,3] These tasks supported Volume X, Sequence Analysis, of NSSR-2. An overview of the work to identify ITER accident sequences was given at the recent Symposium on Fusion Engineering.[4]

The ITER MLD is a large tree structure, spanning seventeen pages. As an example, one branch of the MLD is shown in Figure 10. An interesting issue for ITER is that by modeling the primary and secondary confinement boundaries, an AND gate is introduced into the tree. This gate leads to combinations of failure events. Events listed on both sides of an AND gate are very important since that one event can fail both barriers.

The FMEAs for the cryoplant and cryodistribution showed that only two events are important to public safety—the system rupture and the large release, due to the mass of cryogen involved with these releases. The designers have estimated that the largest single release from the cryoplant is 400 m^3 of liquid helium. Future work will determine if there is any public safety hazard at the site boundary from such large releases.

A new area for risk assessment is studying personnel safety. In the U.S., a new regulation on personnel safety in the Department of Energy[5] has prompted researchers to study these safety issues more closely. Personnel safety studies also support the NSSR-2 volume on occupational safety. One safety issue of interest studied in FY 1997 was personnel safety near large vacuum reservoirs.[6] In the past, the fundamental principles of time, distance, and protective barriers were used to protect workers from vacuum hazards. In ITER, reducing personnel time near maintenance tunnels, as well as using protective barriers, may be difficult. Fortunately, the tunnel mouths form a natural exclusion area that provides some distance to keep workers removed from possible vacuum breaches of

the tunnel to the cryostat vacuum. An independent safety research task performed during the fiscal year was a review of lift truck safety issues.[7] These industrial trucks are used extensively in the construction and operation of research facilities to move supplies and equipment items. ITER and other fusion experiments will use these lift trucks. In the future, the risk assessment area will expand to include more operational safety issues to support construction and operation of ITER and other experiments.

Phenomenological studies. While ITER home teams are experimenting with divertor configurations to find an adequate design solution, divertor off-normal conditions have not yet been fully addressed. An effort to test divertor response to loss of flow events is under way at Sandia National Laboratory using a 30 kW electron beam test facility.[8] Work has been performed to estimate the time to ITER divertor tube burnout under simulated loss of flow accident (LOFA) conditions. For the two sets of tests completed thus far, the pre-LOFA water flow velocity has the largest influence on the time to tube burnout. This timing information is crucial to ensure that the typical ITER divertor plate can be built to cope with the thermal challenges of a LOFA, or protected so that the effects of a LOFA are mitigated by engineered safety features.

The experimental data collected thus far are not statistically robust, so additional LOFA experiments are planned. These new experiments feature two divertor tube mockups: one with a swirl tape insert (the current ITER design) and one without. Both mockups are heavily instrumented with thermocouples so that more information on the heat transfer response during the LOFA can be acquired. One of the goals of this second set of experiments is to improve LOFA modeling. Previous modeling efforts with the first set of data resulted in very poor agreement and the new experiments should improve the data.

Future Activities

Work will continue to support the ITER JCT and the U.S. home team with risk analysis, including initiating event and accident sequence identification, failure modes and effects analysis, component failure rate and repair rate estimation and compilation, and any other risk or safety-related issues that require attention. One such issue is equipment qualification. Support will continute for the NSSR-2 and any other safety documentation that the JCT requires.

If resources permit, additional work in reliability data analysis of data generated at the Tritium Systems Test Assembly will be performed. Aspects of risks to operations and maintenance personnel will be investigated by constructing a master logic diagram for ITER personnel safety as a joint effort with other home teams.

The work on divertor tube LOFA testing with the swirl tape and bare copper tubes is scheduled for completion in mid-FY 1998. After that, Sandia National Laboratories will determine if additional testing will be conducted.

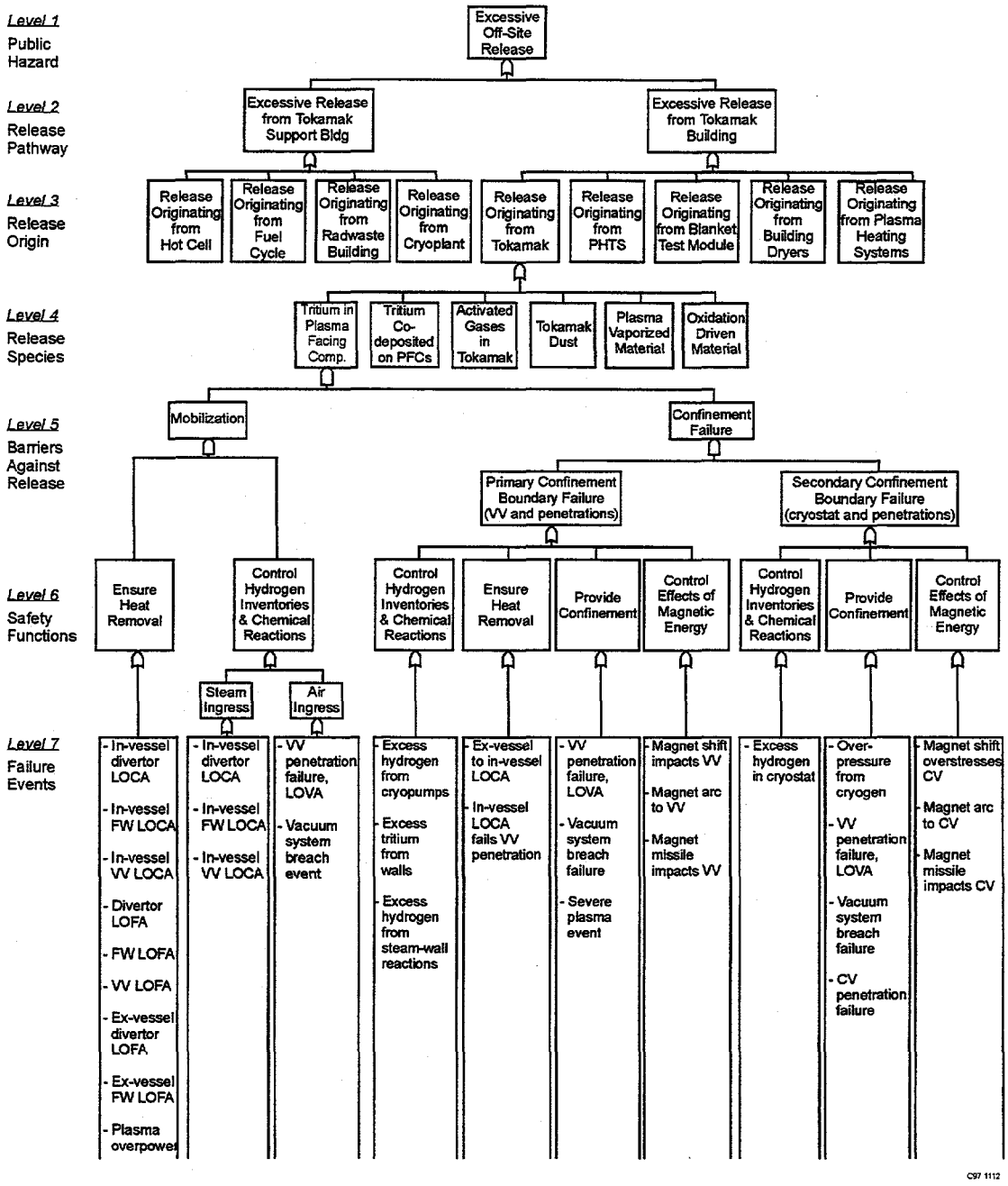

Figure 10. Interim master logic diagram with the 'tritium in plasma facing components' branch expanded to level 7.

References

1. L. C. Cadwallader, *Preliminary Master Logic Diagram for ITER Operation,* Engineering Design File ITER/US/97/EN/SA-07, September 4, 1997.

2. L. C. Cadwallader, *Preliminary Cryoplant FMEA,* Engineering Design File ITER/US/97/EN/SA-05, September 19, 1997.

3. L. C. Cadwallader, *Preliminary Cryodistribution FMEA,* Engineering Design File ITER/US/97/EN/SA-06, September 19, 1997.

4. N. P. Taylor, A. E. Poucet, L. C. Cadwallader, R. Caporali, and C. Girard, "Identification of Postulated Accident Sequences in ITER," presented at the *17th Symposium on Fusion Engineering, San Diego, California, October 6-10, 1997.*

5. U.S. Department of Energy, Order 440.1, *Worker Protection Management for DOE Contractor Employees*, change 1, October 26, 1995.

6. L. C. Cadwallader and C. S. Miller, *Potential Vacuum Hazard to Maintenance Workers and Proposed Solutions for a Cryostat Air Ingress Accident in an ITER Maintenance Tunnel,* Engineering Design File ITER/US/97/EN/SA-04, September 3, 1997.

7. L. C. Cadwallader, *Lift Truck Safety Review,* INEEL/EXT-97-00178, March 1997.

8. T. D. Marshall, R. D. Watson, J. M. McDonald, L. S. Wold, D. L. Youchison, and L. C. Cadwallader, *Experimental Time to Burnout of A Prototypical ITER Divertor Plate During a Simulated Loss of Flow Accident,* SAND96-2611, November 1996.

FUSION SAFETY COMPUTER CODE DEVELOPMENT

Researchers: B. J. Merrill, K. E. Carlson, R. L. Moore, D. A. Petti, S. T. Polkinghorne—INEEL
M. L. Corradini, R. Duckworth, and T. Utschig—UW

Fusion experiments, and eventually fusion power plants, will generate or contain radioactive material in the form of activation products and tritium. These facilities will have a variety of energy sources that can mobilize these materials in several different forms during loss of vacuum accidents (LOVAs), loss of cooling accidents (LOCAs), or plasma disruptions. These energy sources include fusion neutron and particle heat, structure decay heat, plasma-stored thermal and magnetic energy, coolant pressurization, chemical reactions, hydrogen production, and possible combustion. The mobilized forms radioactive material can take are (1) dust resulting from plasma-facing-component (PFC) erosion during normal operation, which can contain tritium or activation products; (2) aerosols resulting from structure surface oxidation; (3) aerosols resulting from PFC erosion during plasma disruptions; (4) isotopic exchange of tritium from PFCs with spilt coolants; and (5) cooling system corrosion products. The extent to which these materials can be confined, and thereby the amount of radio-active material released to the environment reduced, will depend on the degree to which the integrity of confinement barriers can be maintained during LOVAs, LOCAs, and plasma disruptions.

The objective of this task is to obtain, modify, or develop safety computer codes capable of analyzing these events. Several codes are now being pursued: ATHENA, CHEMCON, DSTAR, and MELCOR.[1-4] The following paragraphs describe progress made during FY 1997.

Major Accomplishments

The major accomplishments this fiscal year dealt primarily with the development and verification of models for the MELCOR code and the application MELCOR to ITER safety analyses. The MELCOR code was developed to predict the consequences of hypothetical accidents, such as LOCAs, by predicting the non-equilibrium transport of the liquid and vapor phases of water and the transport of aerosols by this water. ITER will contain radioactive material in the form of activation products and tritium, and will have a variety of energy sources that can mobilize these materials during LOCAs.

Code Development. Three major code development and verification efforts were completed for MELCOR this fiscal year, and two other efforts were begun. First, an enclosure radiant heat transfer model was added to the MELCOR code.[5] This model allows for the direct exchange of radiant power between heat structures located in a common control volume, and for the presence of an atmosphere between these heat structures that can absorb and re-radiate this power. The equations of this model are those solved by the CONTAIN code radiant

heat transfer model.[6] A verification study for this new capability demonstrates that this model obtains the correct results for a standard example problem from Reference 7, and compares well with a transient simulation performed with the CONTAIN code.

Second, modifications were made to the nucleate boiling heat transfer package for water flowing in heated pipes that were added to MELCOR in FY 1996.[8] This heat transfer package contains the Chen[9] equations for nucleate boiling heat transfer and the Biasi[10] correlation for critical heat flux. The Roshenow[11] pool boiling heat transfer correlation was added to this package for low-flow conditions, and the transition film boiling logic of this package was changed this year. A verification study that compares the results for an ITER first wall loss-of-flow accident (LOFA) for this heat transfer package was completed. This verification demon-strated good agreement between MELCOR and ATHENA predictions for this accident.

The third effort was participation in the first phase of an ITER JCT computer code validation study this year. This validation study involved computer codes used for accident analyses reported in the ITER Non-site Specific Safety Report (NSSR-2),[12] and used data obtained from the Japanese ITER Home Team Ingress of Coolant Event (ICE) and Loss of Vacuum Accident (LOVA) experimental facilities.[13] The ICE facility is an experiment in which a high pressure jet of heated water is injected into an evacuated test vessel. The water jet impinges on a heated target plate within the test vessel, and this vessel is connected to a blowdown tank by a pressure-actuated relief valve. Multiple temperature, pressure, and flow measurements are made in this facility. Several ICE pretest calculations were performed with the MELCOR code.[14] These pretest calculations under-predicted vacuum vessel pressurization rates because boiling on the target plate was not accounted for. When the MELCOR ICE model was re-nodalized so that heat transfer between the liquid jet and the target plate was being simulated, MELCOR calculations were found to be in much better agreement with the experimental data.[15]

The LOVA facility consists of a single evacuated vessel with several fast-acting valves that will allow the rapid ingress of air into the vessel. Mass, temperature, and pressure measurements are made in this facility. In addition, the facility has the capability of studying aerosol suspension and re-deposition during an air ingress experiment. The MELCOR results for the LOVA experiments were in reasonable agreement with the data.[16] Four pretest calculations were performed for LOVA. In each case, the evacuated vessel rapidly filled with air when the breach opened. A buoyancy-driven, countercurrent flow was then established (for the 100°C experiments in particular) with cool air flowing into the test vessel and warm air flowing out into the test room.

The addition of lithium and associated physio-chemical phenomena to MELCOR is currently underway. The following modifications will be made: (1) a low pressure melt ejection (LPME) model for the metal in the fuel dispersal interaction (FDI) package will model leaks into a water pool; (2) a high pressure melt ejection (HPME) model for

the metal in the FDI package will model metal sprays into control volume atmospheres; (3) the cavity package (CAV) will model the water leakage into the metal pool; and (4) the CAV package will also model a metal pool interaction with control volume and its atmosphere.

A cryogenic facility recently built at the University of Wisconsin will be used for water-liquid helium experiments. These experiments will provide data that will allow MELCOR to model helium-water interactions.

Code Application. Nine different accident scenarios were analyzed for the ITER NSSR-2 with the MELCOR code this year.[17] These accident scenarios involved the ingress of air or water into the cryostat, and LOCAs in the first wall (FW) primary heat transport system (PHTS). The cryostat is the secondary radioactive material confinement barrier of the ITER device. To investigate the robustness of this confinement barrier, unlikely (frequency 10^{-2} to 10^{-4}/yr) and extremely unlikely (frequency between 10^{-4} to 10^{-6}/yr) ingress of air and water events were examined for the ITER cryostat.

Cryostat air ingress accidents are unlikely events, resulting from postulated breaches of the cryostat boundary, such as a metal bellows failure at a cryostat penetration. The consequences of these accidents are increased heat and weight loads for magnets due to air condensation and a partial vacuum developing in adjoining rooms to the cryostat.

Pressures from an air ingress accident scenario for a postulated 1.0 m^2 cryostat break are shown in Figure 11, which contains the predicted cryostat, cryostat space room, and crane hall pressures. The cryostat space room is an adjoining room to the cryostat. The pressure of the cryostat space room drops to 90 kPa in 1.7 seconds following the initiation of the cryostat breach. This causes the vacuum breakers between the cryostat space room and crane hall to open, and the cryostat space room pressure to drop more slowly reaching a minimum pressure of 82 kPa by 225 seconds. From this point, the cryostat space room pressure begins to rise as it comes into near equilibrium with the cryostat pressure by 400 seconds. The cryostat pressurization rate was limited by the magnets, which condense the air that enters the cryostat through the breach. A peak pressure of 108 kPa is reached in the cryostat and cryostat space room by 965 seconds. These pressures subsequently decay to about 100 kPa by 2,050 seconds. The crane hall pressure drops to 90 kPa by 315 seconds, but recovers to 100 kPa after the vacuum breakers reseat at 400 seconds. The cryostat, cryostat space room, and crane hall pressures are well within the design limits for these enclosures.

The total condensed air mass on the magnets for this study is 7,615 kg by 14,140 seconds. This condensed air mass and the increased heat loads associated with the air are not safety concerns for the magnets.

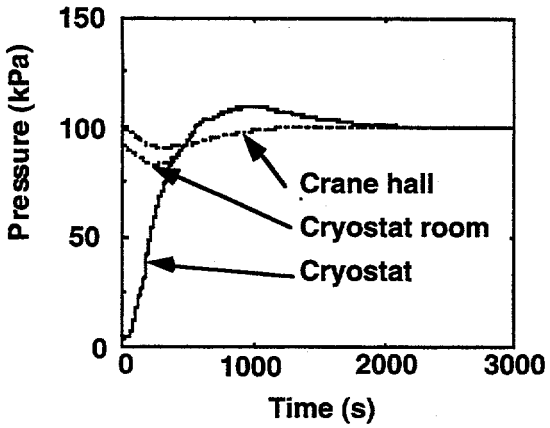

Figure 11. Pressures for the cryostat air ingress accident scenario.

The vacuum vessel (VV) is the primary radioactive material confinement barrier of the ITER device. To examine the robustness of the ITER primary confinement barrier (vacuum vessel plus penetrations), three extremely unlikely LOCAs were analyzed for the ITER design with the MELCOR code.

First, a postulated extremely unlikely event that initiates a large in-vessel LOCA is a vertical displacement event (VDE) for the plasma during which the plasma drops downward, contacting both the inner and outer FW in the lower part of the machine, causing FW pipe damage during a plasma burn. A large number of FW modules around the circumference of the machine are postulated to fail in this event, resulting in a total break area of 0.6 m^2. The resulting vacuum vessel pressure for this event is shown in Figure 12. This pressure exceeds 110 kPa, the actuation pressure for the bleed lines to the vacuum vessel pressure suppression system (VVPSS), by 1.5 s. The VVPSS pressure relief ducts open at 2.8 s after the VV pressure exceeds 200 kPa. The peak VV pressure of 380 kPa occurs at 18 s.

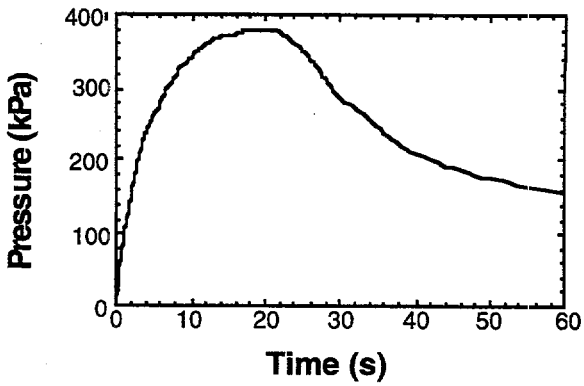

Figure 12. Vacuum vessel pressure during a large in-vessel LOCA in ITER.

This pressure is less than the VV design pressure of 500 kPa.

Second, a postulated ex-vessel LOCA was examined that is a double-ended pipe rupture of the largest pipe (0.3425 m^2 area) in one of the four outboard baffle/limiter (OB/LIM) primary coolant loops during a plasma burn. In this event coolant from the loop will be discharged into the primary heat transport system (PHTS) upper vault. It is assumed that the fusion power will be terminated based on a signal from a pressure sensor in this vault. At the end of the plasma burn, it is assumed that ten coolant tubes (total break area = 0.00157 m^2) in the same PHTS will fail allowing coolant to flow into the plasma chamber. Given the size of these breaks and the water inventory of an OB/LIM loop, this accident represents an enveloping ex-vessel LOCA. Figure 13 shows the upper vault and vacuum vessel pressure for this event. The maximum upper PHTS vault pressure is approximately 160 kPa and occurs 130 seconds into the transient. This peak pressure is below the vault design pressure of 260 kPa.

Finally, a third extremely unlikely accident studied was a double-ended rupture

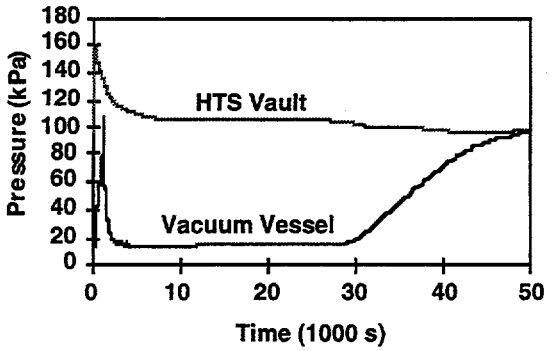

Figure 13. Vacuum vessel and PHTS vault pressures during an ex-vessel LOCA in ITER

of a single in-vessel FW tube during a plasma burn ($1.57x10^{-04}$ m^2 total area). As the pressure builds in the vacuum vessel, a vacuum vessel penetration line (0.02-m^2 cross-sectional area) into an adjoining room designated as the "generic bypass room (GBR)" is assumed to fail as a result of the 100 kPa steam pressure in the vacuum vessel. At issue is the mobilization and possible release of the radioactive inventories contained within the VV. The radiological source terms involved are corrosion products in the coolant and tritium and activated dust inside the plasma chamber. The corrosion product aerosol mass mobilized was 0.13 kg. The mass of tritium mobilized as HTO was 1.4 kg, with 0.8 kg mobilized immediately and 0.6 kg mobilized over a 6-hour time period. The activated dust mass mobilized was 110 kg. For this accident, 22.5 grams of HTO, 14.5 grams of corrosion products, and 111.0 grams of the dust mobilized during this event are eventually released to the environment. These releases are a factor of five or more below the release limits defined for ITER extremely unlikely events.

Future Activities

During the upcoming fiscal year, modifications to MELCOR will be made to better model the behavior of aerosols present during hypothetical thermal-hydraulic accidents such as LOCAs and LOVAs. The liquid metal modules for MELCOR will be completed and used for analysis of the U.S. lithium test blanket module for ITER. The helium-water experiments will begin at the University of Wisconsin.

References

1. K. E. Carlson, P. A. Roth, and V. H. Ransom, *ATHENA Code Manual, Volume 1 and 2*, EGG-RTH-7397, September 1986.

2. M. J. Gaeta, *Chemcon User's Manual*, EGG-FSP-11307, June 1994.

3. B. J. Merrill and S. C. Jardin, "DSTAR: A Comprehensive Tokamak Resistive Disruption Model For Vacuum Vessel Components," *Fusion Engineering and Design*, Vol. 5, 1987, pp. 235-249.

4. R. M. Summers, R. K. Cole, Jr., E. A. Boucheron, M. K. Carmel, S. E. Dingman, J. E. Kelly, *MELCOR 1.8.0: A Computer Code for Nuclear Reactor Severe Accident Source Term and Risk Assessment Analyses*, NUREG/CR-5531 and SAND90-0364, January 1991.

5. B. J. Merrill, *An Enclosure Thermal Radiation Heat Transport Model for the MELCOR code,* Engineering Design File ITER/US/97/TE/SA-04, January 31, 1997.

6. K. E. Washington, et al., "Reference Manual for the CONTAIN 1.1 Code for Containment Severe Accident Analysis," NUREG/CR-5715, May 1991.

7. Siegel, J. R. Howell, *Thermal Radiation Heat Transfer, Third Edition*, Washington, DC, Hemisphere Publishing Company, 1992, pp. 263-278.

8. R. L. Moore, *Documentation of New MELCOR Flow Boiling, EOS, and Diffusion Coefficient Subroutines*, Engineering Design File ITER/US/97/TE/SA-6, May 12, 1997.

9. J. C. Chen, "A Correlation for Boiling Heat Transfer to Saturated Fluids in Convective Flow," ASME Paper, no. 63-HT-34.

10. L. Biasi, et al., "Studies on Burnout," Part 3, *Energia Nucleare*, Vol. 14, (9), 1967, pp. 530-536.

11. J. G. Collier, *Convective Boiling and Condensation*, Second Edition, New York: McGraw-Hill, Inc., New York, 1981, p. 126.

12. H-W. Bartels, editor, *Accident Analysis Specifications for NSSR-1 (AAS), Version 1.2,* S 81 RE 4 96-03-12 W1.1, SEHD 8.1.C-1, ITER Program, May 31, 1996.

13. L. Topilski, *Summary of the ICE/LOVA pre-test calculations,* S 84 MD 20 97-06-06 W 0.1, ITER Program, July 16, 1997.

14. S. T. Polkinghorne, *MELCOR Pretest Predictions of the ICE Experiments*, ITER/US/96/TE/SA-22, November 18, 1996.

15. S. T. Polkinghorne, *Preliminary Post-Test Analysis of ICE Experiments using MELCOR,* Engineering Design File ITER/US/97/TE/SA-9, March 18, 1997.

16. S. T. Polkinghorne, *Pretest Predictions of ICE and LOVA Experiments using MELCOR,* Engineerng Design File ITER/US/97/TE/SA-10, March 24, 1997.

17. D. A. Petti et al., *US Accident Analysis Results for input to the ITER Non-site Specific Safety Report (NSSR-2),* Engineerng Design File ITER/US/EN/SA-03, August 15, 1997.

APPENDIX A

Abstracts or Summaries of Fusion Safety Program Publications

CHEMICAL REACTIVITY OF FUSION MATERIALS

BET Surface Area Measurements of Materials for Fusion Safety Studies

G. R. Smolik, R. A. Anderl, R. J. Pawelko, W. J. Carmack, P. B. Hembree and M. A. Oates, *17th IEEE/NPSS Symposium on Fusion Engineering, San Diego, California, October 6-9, 1997.*

The reaction of air or steam with plasma facing materials and Tokamak dust is a concern during an accident involving a breach in the vacuum plasma chamber of a fusion reactor. Hydrogen generated from steam reactions must be maintained below explosive concentrations. An important parameter influencing reaction rates is the specific surface areas (SSAs) of the materials. We present in this report the capabilities and background that we have obtained using the BET gas adsorption method on various materials. The purposes are to provide correlations with steam reaction rates and to use the method to characterize irradiated beryllium and dust collected from tokamaks.

Steam Chemical Reactivity for Irradiated Beryllium

R. A. Anderl, K. A. McCarthy, M. A. Oates, D. A Petti, R. J. Pawelko, and G. R. Smolik, *Third IEA International Workshop on Beryllium Technology for Fusion, Sangyou Kaikan, Mito City, Japan, October 22-24, 1997.*

This paper reports the results of an experimental investigation to determine the influence of neutron irradiation effects and annealing on the chemical reactivity of beryllium exposed to steam. The work entailed measurements of the H_2 generation rates for unirradiated and irradiated Be and for irradiated Be that had been previously annealed at different temperatures ranging from 450°C to 1200°C. H_2 generation rates were similar for irradiated and unirradiated Be in steam-chemical reactivity experiments at temperatures between 450°C and 600°C. For irradiated Be exposed to steam at 700°C, the chemical reactivity accelerated rapidly and the specimen experienced a temperature excursion. Enhanced chemical reactivity at temperatures between 400°C and 600°C was observed for irradiated Be annealed at temperatures of 700°C and higher. This reactivity enhancement could be accounted for by the increased specific surface area resulting from development of a surface-connected porosity in the irradiated-annealed Be.

Steam Chemical Reactivity for Irradiated Beryllium

R. A. Anderl, K. A. McCarthy, M. A. Oates, D. A. Petti, R. J. Pawelko, and G. R. Smolik, *8th International Conference on Fusion Reactor Materials, Sendai, Japan, October 26-31, 1997*, to be published in *Journal of Nuclear Materials.*

This paper reports experimental results concerning the influence of neutron irradiation effects and annealing on the chemical reactivity of beryllium exposed to steam. The work entailed: (1) measurements of swelling, porosity, and specific surface area for irradiated Be annealed at temperatures ranging from 700°C to 1200°C and (2) measurements of hydrogen generation rates for unirradiated Be, irradiated

Be, and irradiated-annealed Be exposed to steam at elevated temperatures. For irradiated Be, volumetric swelling increased from 14% at a 700°C anneal to about 56% at a 1200°C anneal. Gas-release measurements during annealing indicated the development of a surface-connected porosity network. Specific surface areas for irradiated-annealed Be increased with the anneal temperature. Steam-chemical reactivity was similar for irradiated and unirradiated Be at temperatures between 450°C and 600°C. For irradiated Be exposed to steam at 700°C, the reactivity accelerated rapidly and the specimen experienced a temperature excursion. Irradiated-annealed Be showed enhanced chemical reactivity related to its higher specific surface area.

ACTIVATION PRODUCTS MOBILIZATION AND TRANSPORT

Collection and Analysis of Particulate from the DIII-D Tokamak

W. J. Carmack, K. A. McCarthy, D. A. Petti, A. G. Kellman, and C. P-C. Wong, *Fourth International Symposium on Fusion Nuclear Technology, Tokyo, Japan, April 7-11, 1997*, to be published in *Fusion Engineering and Design*.

Particulate (i.e. tokamak dust) has been collected from the DIII-D tokamak located at General Atomics in San Diego, California, USA. Two methods were used to collect particulate with the goal of preserving the particle size distribution and physical characteristics of the particulate. Vacuum collection on substrates and adhesion removal with metallurgical replicating tape were chosen as non-intrusive sampling methods. Sampling was completed in four areas of the machine; the 0 to 90° area, the 90 to 180° area, the 180 to 270° area, and the 270 to 360° area. The 0° direction designates the north side of the DIII-D machine. Four tiles in each area were sampled: the first vertical tile above the floor on the center-post, a floor tile next to the center post, a tile on the isolated ring, and the first tile up from the isolated ring on the divertor. In addition samples were collected from underneath the floor tiles in the 275° and the 75° location and from inside the neutral beam injection ports. The count median diameter of the samples ranged from 0.50 to 0.86 microns with geometric standard deviations ranging from 2.0 to 3.5. Diameters of average mass calculated from Hatch-Choate equations based upon log normal distribution characteristics ranged from 2.8 to 7.5 microns.

The Safety Implications of Tokamak Dust Size and Surface Area

K. A. McCarthy, D. A. Petti, W. J. Carmack, and G. R. Smolik, *Fourth International Symposium on Fusion Nuclear Technology, Tokyo, Japan, April 7-11, 1997*, to be published in *Fusion Engineering and Design*.

Tokamak dust, accumulated primarily from sputtering and disruptions, has important safety issues associated with it. The dust may contain tritium, it may be activated, and it may be chemically toxic and chemically reactive. The size of the dust and the surface area are important parameters in determining potential hydrogen production and transport of activated/chemically toxic dust. In this paper we examine the effect of the size distribution of the dust on these safety issues.

Hydrogen Generation from Steam Reaction with Tungsten

G. R. Smolik, K. A. McCarthy, D. A. Petti, and K. Coates, presented at the *Eighth International Conference on Fusion Reactor Materials, Sendai, Japan, October 26-31, 1997*, to be published in *Journal of Nuclear Materials*.

A LOCA in a fusion reactor involving an ingress of steam presents a safety concern due to hydrogen generated from steam reactions with plasma-facing components. Hydrogen concentrations must be maintained below explosive levels. To support safety evalua-tions we have experimentally determined hydrogen gene-ration rates when a tungsten alloy is exposed to steam from 400 to 1200°C. Our study

included effects of steam pressure (0.28 to 0.84 atmosphere) and gas velocity (0.011 to 0.063 m/s). In this paper we present relationships for the reaction rates and oxidation phases and mechanisms associated with the hydrogen generation.

Experimental Investigation of Disruption-Induced Aerosol Mobilization in Accident Scenarios of ITER

J. P. Sharpe, M. Bourham, J.G. Gilligan, *17th IEEE/NPSS Symposium on Fusion Engineering, San Diego, California, October 6-9, 1997.*

Electrothermal (ET) plasma sources, such as the SIRENS facility at North Carolina State University, have been used to simulate disruption heat loads because magnitudes and physical mechanisms of heat transfer in the ET source are similar to those in a tokamak disruption. Changes to the SIRENS facility at NCSU have allowed experiments in which material is vaporized within the ET source and allowed to expand into a large chamber. This expansion generates aerosol particles in a fashion similar to those expected from hard disruptions expected in ITER. Particulate of ITER-relevant metals (copper, stainless steel 316, tungsten, and aluminum) in the size range of 0.075 to 25 μm have been produced in SIRENS in a simulated disruption heat load of 2.8 MJ/m^2 over a 50 μs heat pulse. Particle size distributions have been determined and are presented in this paper.

Mobilization from Austenitic Stainless Steel in Air and Steam: Recent Tests, Compilation of Data from Tests to Date, and Resulting Dose Calculations

G.R. Smolik, K.A. McCarthy, W.J. Carmack, and K. Coates, paper presented at the *17th IEEE/NPSS Symposium on Fusion Engineering, , San Diego, California, October 6-9, 1997.*

A failure in the vacuum plasma chamber of a fusion reactor could result in the intrusion of air or steam causing oxidation of activated materials comprising plasma facing and structural components. Oxides formed may then be mobilized by mechanisms involving either volatilized or spalled oxides. We have measured the mobilization of various elements from austenitic stainless steels, which is a candidate structural material, using transpiration test methods. This paper compiles all data for this type of alloy from our experimental studies performed from 1983 to 1996 and presents dose calculations resulting from the updated database.

DIII-D Dust Particulate Characterization

W. J. Carmack, M. E. Engelhardt, P. B. Hembree, K. A. McCarthy, and D. A. Petti, INEEL/EXT-97-00702, November, 1997.

Tokamak dust is a key component of the ITER accident source term. Understanding the amount of dust expected in ITER and its physical and chemical characteristics is needed to verify conservative assumptions currently used in ITER safety analyses. An important part of this safety research and development work is to characterize dust from existing tokamaks. In this engineering design file, we present the collection and data analysis methods used and the particle size distribution of dust particulate collected on the lower surfaces of the first wall and from beneath two floor tiles of the DIII-D vacuum vessel. The collected particulate was analyzed at the Idaho National Engineering and Environmental Laboratory (INEEL).

Tritium and Helium Retention and Release from Irradiated Beryllium

R. A. Anderl, G. R. Longhurst, M. A. Oates and R. J. Pawelko, *Third IEA International Workshop on Beryllium Technology for Fusion, Sangyou Kaikan, Mito City, Japan, October 22-24, 1997.*

This paper reports the results of an experimental effort to anneal irradiated beryllium specimens and characterize them for steam-chemical reactivity experiments. Fully-dense, consolidated powder metallurgy Be cylinders, irradiated in the EBR-II to a fast neutron (>0.1MeV) fluence of ~$6x10^{22}$ n/cm^2, were annealed at temperatures from 450°C to 1200°C. The releases of tritium and helium were measured during the heat-up phase and during the high-temperature anneals. These experiments revealed that, at 600°C and below, there was insignificant gas release. Tritium release at 700°C exhibited a delayed increase in the release rate, while the specimen was at 700°C. For anneal temperatures of 800°C and higher, tritium and helium release was concurrent and the release behavior was characterized by gas-burst peaks. Essentially all of the tritium and helium was released at temperatures of 1000°C and higher, whereas about 1/10 of the tritium was released during the anneals at 700°C and 800°C. Measurements were made to determine the bulk density, porosity, and specific surface area for each specimen before and after annealing. These measurements indicated that annealing caused the irradiated Be to swell, by as much as 14% at 700°C and 56% at 1200°C. Kr gas adsorption measurements for samples annealed at 1000°C and 1200°C determined specific surface areas between 0.04 m^2/g and 0.1 m^2/g for these annealed specimens. The tritium and helium gas release measurements and the specific surface area measurements indicated that annealing of irradiated Be caused a porosity network to evolve and become surface-connected to relieve internal gas pressure.

RISK ASSESSMENT

Lift Truck Safety Review

L. C. Cadwallader, INEEL-EXT-97-00178, March 1997.

This report presents safety information about powered industrial trucks. The basic lift truck, the counterbalanced sit down rider truck, is the primary focus of the report. Lift truck engineering is briefly described, then a hazard analysis is performed on the lift truck. Case histories and accident statistics are also given. Rules and regulations about lift trucks, such as the U.S. Occupational Safety and Health Administration laws and the Underwriter's Laboratories standards, are discussed. Safety issues with lift trucks are reviewed, and lift truck safety and reliability are discussed. Some quantitative reliability values are given.

Identification of Postulated Accident Sequences in ITER

N. P. Taylor, A. E. Poucet, L. C. Cadwallader, R. Caporali, and C. Girard, presented at the *17th Symposium on Fusion Engineering, San Diego, California, October 6-10, 1997.*

An essential part of the Engineering Design Activities (EDA) for the International Thermonuclear Experimental Reactor (ITER) is the assurance that the design meets strict safety criteria. Analyses have been performed of postulated accidents, in order that the possible consequences can be assessed against targets for releases and other criteria. The range of events considered is based on studies which use systematic techniques to provide a comprehensive identification of potential accident initiators and sequences. Two independent and complementary approaches have been employed, illustrated here by a portion of a global fault tree and a sample event tree. The result of these studies is a demonstration that the ITER accident analyses treat a comprehensive range of event sequences, and give confidence that the ITER engineering design will achieve its safety targets.

Experimental Time To Burnout of A Prototypical ITER Divertor Plate During a Simulated Loss of Flow Accident

T. D. Marshall, R. D. Watson, J. M. McDonald, L. S. Wold, D. L. Youchison, and L. C. Cadwallader, SAND96-2611, November 1996.

The Loss of Flow Accident (LOFA) is a serious safety concern for the International Thermonuclear Experimental Reactor (ITER) because it has been suggested that greater than 100 s are necessary to safely shut down the plasma when ITER is operating at full power. In this experiment, the thermal response of a prototypical ITER divertor tube during a simulated LOFA was studied. The divertor tube is fabricated from oxygen-free high-conductivity copper to have a square geometry with a circular coolant channel. The inner diameter of the coolant channel is 0.77 cm, the heated length is 4.0 cm, and the heated width is 1.6 cm. The mockup does not feature any flow enhancement techniques, i.e., swirl tape, porous coating, or

internal fins. One-sided surface heating of the mockup is accomplished through the use of the 30-kW Sandia Electron Beam Test System. After reaching steady-state temperatures in the mockup, as determined by two K-type thermocouples embedded 0.5 mm beneath the heated surface, the circulation pump for the high-temperature, high-pressure coolant loop is manually tripped off and the coolant flow allowed to naturally coast down. Electron beam heating continues after the pump trip until the divertor plate's heated surface exhibits the high-temperature transient normally indicative of rapidly approaching "burnout." Experimental data show that time-to-burnout increases proportionally with increases in the initial (before the pump trip) inlet velocity and decreases proportionally with increases in the incident heat flux.

APPENDIX B

Abstracts of Fusion Safety Program ITER Engineering Design Files

Hydrogen Generation During Steam Oxidation of a Tungsten Alloy

G. Smolik, ITER/US/97/TE/SA-2, January 31, 1997.

This Engineering Design File (EDF) presents experimental results of hydrogen generation produced during the oxidation of a tungsten alloy in steam from 400 to 1200°C. We had obtained estimates of hydrogen production from measurements of alloy recession from tests performed in 1988-89. We have since improved our experimental methods and measure hydrogen generation with a gas chromatograph. The current tests have been made in environments with steam pressures between 0.28 and 0.84 atm. and gas velocities (steam plus argon) between 0.011 m/s (66 cm/min) and 0.063 m/s (376 cm/min.) to investigate the influences of these parameters upon hydrogen generation.

We found a linear Arrhrenius relationship for hydrogen generation rate from 500 to 1200°C. This relationship shown as follows is for our baseline test conditions, i.e., a steam pressure of 0.84 atm. and a gas velocity of 0.037 m/s.

$$\text{Rate [liters } H_2\text{(STP)/m}^2\text{-s]} = 15{,}140\ [\exp(-16{,}720/T)]$$

We found that steam pressure and gas velocity both influenced hydrogen generation. Hydrogen generation is related to steam pressure by $P^{(0.78)}$ when gas velocity is held constant at 0.011 m/s and to gas velocity by $V^{(0.55)}$ when steam pressure is maintained near the ambient pressure of 0.84 atm. We combined these relationships into a general equation shown below. The coefficient has been determined for steam pressure and gas velocity represented in units of (atm) and (m/s), respectively. The equation predicts our experimental data over the entire test range within 35 percent. We recommend it for use in safety calculations but caution that the velocity term may apply only for laminar flow since these are the conditions that prevailed during all of our tests.

$$\text{Rate [liters } H_2\text{(STP)/m}^2\text{-s]} = (1.02\text{x}10^5)^* [P]^{(0.78)*} [V]^{(0.56)*} [\exp(-16{,}720/T)]$$

We used X-ray diffraction (XRD) to identify residual and transported oxides for samples tested at 1000°C. We could not find any evidence of WO_2. The oxides were mostly WO_3 or sub-stoichiometric oxides of this phase, e.g., $WO_{2.9}$, or mixed transition metal-tungsten oxides, such as $CoWO_4$ or $FeWO_4$. The latter phases were left as residual porous layers on the samples. This information shows that basically three moles of hydrogen are generated from each mole of tungsten reacted, i.e., the tungsten is oxidized to its highest oxidation state, and the volatilization mechanism involves the formation of some volatile hydroxide or hydrate complex from WO_3. No additional hydrogen is generated from the volatilization process.

Steam-Chemical Reactivity Experiments for Russian TGP-56 Be

R. A. Anderl, ITER/US/97/TE/SA-5, February 27, 1997.

This report documents experiments that have been done at the Idaho National Engineering and Environmental Laboratory to measure hydrogen generation rates for

Russian TGP-56 grade Be cylindrical specimens exposed to steam. These fully-dense specimens were tested at 500, 600, 700 and 800°C, temperatures that provided a means to compare the observed chemical reactivities with those observed in our previous tests for cylindrical Be control specimens. A comparison of the hydrogen generation results indicates that both kinetic hydrogen generation-rate behavior and average hydrogen generation rates are in reasonable agreement for the two types of specimens, especially for temperatures above 600°C. Differences in the hydrogen generation behavior for the two types of specimens at 600°C and below are attributed to possible differences in surface condition, an effect we observed in multiple tests with the Be control specimens

Correlations for Beryllium-Steam Reaction Rates

K. A. McCarthy, ITER/US/97/TE/SA-13, May 20, 1997.

Over the last six years, the Fusion Safety Program at the Idaho National Engineering and Environmental Laboratory has tested the chemical reactivity of various forms of beryllium in steam; in this engineering design file (EDF), we focus on tests with dense beryllium. Beryllium reacts exothermically with steam to produce hydrogen, a potential safety hazard. Data in beryllium-steam reactions are necessary to support safety analyses of the International Thermonuclear Experimental Reactor.

The purpose of this EDF is to present curve fits to the compiled data, and recommend which curve fits are to be used for NSSR-2. These curve fits are "interim" fits to be used for the NSSR-2; these data will be revisited before recommendations are made for curve fits to be used in the NSSR. We recommend using the following equation, the fit over data at 600°C and below, for estimating hydrogen production from oxidation of tokamak dust for NSSR-2 calculations.

$$H_2\ Generation\ Rate\left(\frac{L[STP]}{m^2 s}\right) = 302\exp\left(-\frac{13{,}465}{kT}\right)$$

We will do additional testing and data analysis prior to NSSR calculations, and reevaluate this issue. For all other calculations, we recommend using the correlations in the 1996 version of SADL. Because of uncertainties in the irradiated beryllium chemical reactivity at temperatures above 600°C, it does not make sense at this time to recommend new correlations for calculations other than those involving oxidation of tokamak dust.

Steam-Chemical Reactivity Experiments for LANL Plasma-Sprayed Be

R. A. Anderl, ITER/US/97/TE/SA-23, September 1997.

This report documents experiments and analyses that have been done at the Idaho National Engineering and Environmental Laboratory (INEEL) to measure chemical reactivity of plasma-sprayed Be specimens exposed to steam. Test specimens for this work were fabricated at the Beryllium Atomization and Thermal Spray Facility, Los Alamos National Laboratory (LANL). Specimens were of two different densities, 94% and 92% of theoretical density (TD), with nominal dimensions 1.5 cm x 1.5 cm x 0.3 cm. Our approach in this work was primarily twofold; (1) characterization of the density, porosity and specific surface area

for the specimens and (2) measurements of the chemical reactivity of specimens exposed to steam.

Density and porosity characterization was based on liquid immersion density measurements, and BET specific surface areas were measured using a gas-adsorption technique with Kr as the adsorptive gas. The immersion-density measurements gave bulk densities of 94%TD, with an open porosity of 1.4% and a closed porosity of 4.2%, and 92%TD, with 7.7% for open porosity and a statistically insignificant closed porosity. BET measurements and analyses gave specific surface areas of 0.085 m^2/g for the 94%TD PS material and 1.21 m^2/g and 1.07m^2/g for two different specimens of 92%TD PS material. These porosity and surface-area results were compared to corresponding results for Battelle plasma-sprayed Be and for consolidated powder metallurgy (CPM) Be of varying density. For comparable bulk densities and porosity, the plasma-sprayed Be with bulk densities of 92%TD or less had much higher specific surface areas than CPM Be, reflecting a higher surface-area microstructure, i.e., flat splat-like features for PS Be compared to more round-like particles for CPM Be.

Chemical reactivity experiments were performed for the LANL PS Be specimens exposed to steam at temperatures ranging from 350°C to above 1000°C. Hydrogen generation rates and parabolic rate constants were derived from mass-spectrometer measurements and from measurements of specimen weight-gain. These experiments showed a complex Be-steam reactivity behavior, dependent primarily on the test temperature and the specimen open porosity and surface area.. For temperatures of 450°C and less, the kinetics were parabolic. At 500°C, the reactivity was initially parabolic and subsequently became moderately accel-erating as the steam exposure continued. For a temperature of 600°C, the 94%TD PS material exhibited an accelerating behavior and the 92%TD PS material showed a run-away behavior characterized by a large temperature excursion. For temperatures of 700°C and above, the 94%TD PS material showed both accelerating and linear behavior.

Results from the chemical reactivity experiments for the LANL-PS Be material were compared to corresponding results for Battelle PS Be and for fully-dense and porous CPM-Be. At temperatures from 700°C and below, H_2 generation rates for the LANL 94%TD PS Be were about a factor of 100 higher than those for fully-dense CPM Be, however, the rates were significantly lower than those for LANL 92%TD PS Be, Battelle-PS Be and porous CPM-Be. Differences in the H_2 generation rates could be accounted for by the measured differences in surface area for the various materials.

DIII-D Dust Particulate Characterization

W. J. Carmack, ITER/US/97/TE/SA-8, March 1997.

Tokamak dust is a key component of the ITER accident source term. Understanding the magnitude of dust expected in ITER and its physical and chemical characteristics is needed to verify conservative assumptions currently used in ITER safety analysis. An initial part of this safety research and development work is to characterize dust from existing tokamaks. In this engineering design file, we present the collection and data analysis methods used and the particle size distribution of dust particulate collected on the lower surfaces of the first wall and from beneath two floor tiles of the DIII-D vacuum vessel.

Particulate (i.e., tokamak dust) has been collected from the DIII-D tokamak located at General Atomics in San Diego, California, USA. Two methods were used to collect particulate with the goal of preserving the particle size distribution and physical characteristics of the particulate. Choice of collection technique is important because the sampling method used can bias the particle size distribution collected. Vacuum collection on substrates and adhesion removal with metallurgical replicating tape were chosen as nonintrusive sampling methods. Sampling was completed in four areas of the machine: 0 to 90° area, the 90 to 180° area, the 180 to 270° area, and the 270 to 360° area. The 0° direction designates the north side of the DIII-D machine. Four tiles in each area were sampled; the first vertical tile above the floor on the floor on the center-post, a floor tile next to the center post, a tile on the isolated ring, and the first tile up from the 275° and the 75° location and from inside the neutral beam injection ports. The count median diameter of the samples ranged from 0.5 to 0.86 microns with geometric standard deviations ranging from 2.0 to 3.5. Diameters of average mass calculated from Hatch-Choate equations based upon log normal distribution characteristics ranged from 2.8 to 7.5 microns.

Scoping Results of SIRENS for Wall Material Vaporization Studies

M. Bourham and J. P. Sharpe, ITER/US/97/TE/SA-14, June 1, 1997.

This document describes scoping tests conducted in the SIRENS facility. These tests have been conducted prior to performance of experiments to investigate plasma-disruption induced mobilization of activated wall material in ITER. The SIRENS facility has been modified during the interaction of a high-energy density plasma and a test material. The purpose of this document is to present key experimental parameters and quality control procedures associated with the generation of data and results in the SIRENS facility.

An existing electrothermal plasma gun (SIRENS) has been modified to simulate plasma disruption events in terms of power flux and produce mobilized particles in the same manner as expected in ITER. The sleeve section of the SIRENS electrothermal source has been changed to use ITER-relevant materials. An expansion chamber

has been added to allow controlled collection of the resulting particulate. Preliminary tests have been successfully conducted on 316 stainless steel and copper, demonstrating the validity of the experiment in accomplishing the prescribed task. Resulting particle size distributions from scoping tests are reported, as well as insight gained from performing these tests.

Future work for this experiment includes detailed analysis of the condensation results for copper, stainless steel 316, tungsten, carbon, and certain combinations of these materials. After building this experimental database of resulting particle size distributions, modeling will be performed to aid in extrapolation of SIRENS results to ITER conditions.

Fusion Aerosol Source Test (FAST) Air Exposure of 316SS

W. J. Carmack, ITER/US/97/TE/SA-15, May 31, 1997.

This engineering design file presents the results of four air-exposure tests of 316 stainless steel in the FAST facility. The four separate tests were conducted at temperatures of 500, 600, 700, and 800°C. An air volumetric flow rate of 25 standard liters per minute was maintained in the test sections for a duration of 5 hours.

These four tests were conducted to measure the total mobilized material resulting from the air exposure conditions at each temperature. Tests were conducted with procedures outlined in the Performance Test Results engineering design .

We have compared the data obtained in these tests with data from the VAPOR facility at 800°C and with scoping tests completed previously in the FAST facility. Our tests of 316 stainless steel in air in FAST have provided measurements demonstrating the mobilization of certain elements. Mobilization of Mo and Cr showed progressive increases with temperature from 500 to 800°C. Iron and Mn were also found to be mobilized above the EMFV and air background levels without a discernible temperature dependency for temperature from 500 to 800°C. Measurements of all other elements were generally at or below EMVFs.

We obtained higher mass flux measurements of Mo, Cr, Fe, and Mn in VAPOR compared to those from FAST at 800°C. We attribute the higher measurements—up to a factor of about thirty (30) for Fe and Mn—to greater amounts of spalled oxides. More spalled oxide is produced in VAPOR than in FAST due to development of thicker oxides from longer exposures. The thicker layers combined with the specimen size and shape, i.e., sharp corners, and a more rapid cooling rate produce high stress concentrations. More of the spalled oxide will be collected in VAPOR where the test chamber encompasses the specimen than in FAST where particles have a greater likelihood to settle out and be retained in the test section than transported to the collecting media. The measurements of several elements (Mo, Cr, and Ni) show a factor of 3 higher mobilization in VAPOR compared to FAST. We believe that the factor of three difference in mobilization is a fairly good correlation between mobilization in FAST and VAPOR considering that we observe evidence of contributions of oxide spalling to mobilization even in FAST.

The benefits of the air tests in FAST are that we have been able to demonstrate relatively low mobilization rates of certain elements down to 500°C and have been able to reduce detection limits due to the large surface area of the test section. The EMFVs that we use to develop cumulative maximum flux plots have been reduced by factors of 10 to 15 for all elements compared to similar tests in VAPOR.

Revision of DIII-D Quadrant 2 Detail Vacuum Analysis

W. J. Carmack, ITER/US/97/TE/SA-16, July 31, 1997.

Particulate (i.e. tokamak dust) has been collected from the DIII-D tokamak located at General Atomics in San Diego, California, USA. Analysis of the collected particulate has been completed and is documented in Carmack et al. 1997. The count median diameter (CMD) analysis of all of the samples collected from the DIII-D vacuum vessel ranged from 0.5 μm to 0.86 μm with geometric standard deviations (GSDs) ranging from 2.0 to 3.5 with exception of the Quadrant 2 detail vacuum sample. Diameters of average mass calculated from Hatch-Choate equations based upon log normal distribution characteristics ranged from 2.8 to 7.5 μm again with the exception of the Quadrant 2 detail vacuum sample. Previous analysis of the Quadrant 2 detail vacuum sample yielded a CMD of 0.29 μm with a GSD of 6.76.

The purpose of this EDF is to present the revised data analysis of the Quadrant 2 detail vacuum sample. These values were significantly different from those obtained throughout the DIII-D machine in the companion samples collected during the sampling campaign. The CMD value of 0.29 μm was lower than expected and the GSD value of 6.76 was higher than expected indicating that the photographs obtained for the sample were not representative. There is no reason to expect Quadrant 2 samples to vary significantly from samples obtained in other quadrants. Overall the original Quadrant 2 detail vacuum sample did not physically show any indication that it differed from the samples collected from the other three quadrants except for "halos" around large particles in high magnification photographs. It is now known that these halos can be eliminated when acquiring photographs with the microscope and were most likely missed due to inexperience in the analysis process. The original Quadrant 2 detail vacuum sample was the first vacuum sample analyzed with this technique. Because of these halos, accurate particle counts were not obtained from the original photographs. Photographs were retaken and a new analysis completed on the Quadrant 2 detail vacuum sample. This analysis resulted in a CMD of 0.72 μm and a GSD of 2.68, consistent with distributions in the other three quadrants.

We have referred to specific photographs by a designation including an identifier for the microscope objective used. We have referred to photographs taken using the 100x objective as the 100x magnification. In practice, when using the 100x objective, the overall magnification obtained is 1000x because there is a 10x multiplication In the optics of the microscope. We have determined that it is more appropriate to refer to the photographs taken using the 100x objective as the 1000 x photograph. In the past we have referred to photographs by the

objective used to acquire the photograph. This number does not accurately reflect the obtained magnification since there is a 10x lens in the microscope making the true magnification 1000x when using the 100x objective. Hence, analyses presented in this EDF and in future publications will refer to the 1000x, 500x, 200x, 100x, and the 50x magnifications instead of the 100x, 50x, 20x, 10x, and 5x magnifications respectively. This "extra" 10 x is not new, nor does it indicate a change or modification of the analysis procedure, but it is a more accurate representation of the actual magnification used.

C-MOD Dust Particulate Characterization

S. Gorman, W. J. Carmack, and P. B. Hembree, ITER/US/97/TE/SA-17, August 1997.

Analysis of particulate from the Alcator C-MOD tokamak located at Massachusetts Institute of Technology (MIT) in Boston, Massachusetts, has been completed and is documented in this report. The sample obtained from Alcator C-MOD was not originally intended for outside examination. However, Alcator personnel graciously sent a sample to the INEEL for analysis. A commercial vacuum cleaner was fitted with a stainless steel tube onto which a canister containing a 2-μm pore size filter was attached. The entire surface of the plasma facing wall was then vacuumed. This process could not remove all of the finest dust which tended to cling to the surface of the tiles. We believe use of this type of filter resulted in failure to collect small particulate. The sample visibly contained human hair, pieces of paper, and general large pieces of various materials. Upon receipt at the INEEL, the sample was removed from the plastic transportation bag and placed in a metal container. The loose particulate on the filter was tapped off into the container. The residual powder left on the bag surface was washed with high purity water and placed into a vial. The sample placed into the metal container was sieved through a 1.680-mm screen and 250-micron screen to remove the large pieces of materials, such as hair and paper. The resulting sieved sample was then analyzed using an optical microscope, SEM microscope, Microtrac FRA particle size analyzer, and a BET surface area analysis instrument.

The count median diameter (CMD) of the optical analysis samples ranged from 0.61 microns to 1.1 microns with geometric standard deviations (GSD) ranging from 2.8 to 5.2. Mass median diameters (MMD) calculated from the Hatch-Choate equations based upon log normal distribution characteristics ranged from 68 to 176 microns.

Oxidation Driven Mobilization Activation Product Source Term Input for NSSR-2

K. A. McCarthy, ITER/US/97/TE/SA-18, August 14, 1997.

The purpose of this EDF is to provide the oxidation-driven activation product source term to be used by the JCT in preparing input for the Non-site Specific Safety Report (NSSR-2). The source term developed here is based on experiments carried out by the Fusion Safety Program at the Idaho National Engineering and Environmental Laboratory (INEEL). The

spreadsheet used to calculate source term input for ESECS and NSSR-1 was updated to include the activation calculation relevant to NSSR-2. The spreadsheet now contains information for calculating the NSSR-2 tungsten activation product source term in addition source terms for ESECS and NSSR-1. This allows the user to calculate a variety of cases and provides flexibility so that the spreadsheet can be used to calculate new cases if parameters change.

As specified by the ITER JCT task officer for this task, we provide examples of the tungsten activation product source term only (the spreadsheet can also be used to calculate the dose for other ITER-relevant materials such as 316SS and copper, as well as Inconel and vanadium). Calculations for NSSR-2 can be done for three dose scenarios (four types of dose from each scenario: dose from plume passage, early dose, chronic dose without ingestion, and chronic dose with ingestion), one fluence (0.3 MWa/m^2 pulsed fluence at shutdown), and two accident environments (air and steam). Additionally, the user can input his or her own activation calculation and/or dose information.

The source term calculations were verified to the extent possible against other available information, specifically, NSSR-1 and ESECS results.

Characterization of Metal Powder for Use in Japan's LOVA Experiment

W. J. Carmack, ITER/US/97/TE/SA-19, August 19, 1997.

This report contains the analysis and documentation of three different powders analyzed at the INEEL: ALMET (Aluminum Metal), PH13 (iron, chromium, nickel, and molybdenum), and INK718 (Inconel). None of these powders are tokamak dust, but rather fine particle dust given to the Japanese ITER Home Team for use in the LOVA experiments. The ALMET sample, and samples of aluminum metal, iron, chromium, nickel, and molybdenum dust, were made by a rapid spray solidification process at the INEEL. A few grams of each dust were placed in separate pieces of weight paper and from there vacuumed onto their respective filters for sample collection. These samples were then analyzed.

The optical microscope analysis of the ALMET, INK718, and PH13 dusts indicate the count median diameter of all of the samples ranged from 1.27 to 1.38 μm with geometric standard deviation ranging from 1.64 to 1.92. These results indicate a close similarity between these particulate samples.

Samples of each of the dusts were analyzed with the Microtrac FRA particle size analyzer. The measured $d_{50\%}$ (volumetric) values ranged from 3.63 to 5.91 and the GSD ranged from 1.43 to 1.99. The relatively low GSD values obtained from both the optical analysis and the volumetric analysis indicate a narrow distribution.

Characterization of Disruption-Induced Particulate from ITER Relevant Metals

J. P. Sharpe, ITER/US/97/TE/SA-21, November, 1997.

The SIRENS high heat flux facility at North Carolina State University has been used to simulate the erosion and mobilization effects on ITER-relevant materials exposed to hard disruption

conditions. Specifically, size distributions of various particulate resulting from surface vaporization and subsequent condensation under vacuum conditions have been produced. This document presents fundamental data obtained from a set of experiments performed with copper, stainless steel, tungsten, and aluminum (to simulate beryllium).

For this experimental investigation, particulate were generated from test material mobilized in the SIRENS electrothermal source section. Material exiting the source section was then introduced into a large controlled volume (cylindrical glass tube) upon which collection substrates (buttons) were mounted. Selected buttons were observed with a scanning electron microscope (SEM); the buttons generally displayed a significant population of particles deposited on the exposed surface. Using the SEM, photographs of a given button were obtained and analyzed for the number and size of deposited particles. This data was then fit to the log-normal distribution function, generating the overall particle size distribution for the selected button.

Particulate collected and analyzed from the various metals studied in this task displayed count median diameters from 0.3 to 3.0 μm. The minimum and maximum observed particle sizes where 0.075 and 50 μm, respectively. The majority of the particles in the underlying distributions, however, were ~1 μm in diameter.

In the near future, carbon and mixed-material tests will be performed. Later on, modeling of particulate generation and the necessary extrapolation to ITER will also be performed. The database resulting from this experimental task may be used to test models predicting the size of particulate mobilized during possible ITER disruptions.

Mobilization from Austenitic Stainless Steels During Air and Steam Exposures

G. R. Smolik, W. J. Carmack, and K. Coates, ITER/US/97/TE/SA-25, December 1997.

The Fusion Safety Program at the Idaho National Engineering and Environmental Laboratory (INEEL) has been testing materials to measure the mobilization of various species during air and steam exposures for over 10 years. These measurements support off-site dose calculations for postulated accident scenarios. Different procedures based upon transpiration test methods have been used to test austenitic stainless steels, i.e., 316 stainless steel and PCA (primary candidate alloy), a similar alloy with 0.32 wt% titanium, 14.3 wt% chromium, and 16.6 wt% nickel. Earlier tests were performed in VAPOR (Volatilization of Activation Products Oxides Reactor). VAPOR is a system where smaller samples are contained within a quartz test chamber and can be heated either inductively or with a tube furnace. Most of the earlier tests were at higher temperatures, i.e., 800 to 1200°C. However, evolving accident scenarios for ITER required data at lower temperatures. Test methods and analytical procedures were improved and longer tests of up to 100 hours were used to obtain data at lower temperatures. Ultimately, a test facility called FAST (Fusion Aerosol Source Test) was built. This system uses a tubular test section that provided about two orders of magnitude

larger surface area. The larger test section enabled us to obtain measurable mass flux, or smaller EMFVs (engineering maximum flux values), for various elements down to 500°C.

The purpose of this report is to compare and consolidate the data from the various test series on austenitic stainless steels. We have done this and by using committee review have agreed upon data to be used for constructing cumulative maximum flux plots (CMFPs) for various elements for exposures in air and steam. These are the values that we recommend for safety studies involving accidents with ingress of air or steam. From a mechanistic standpoint, we find that particles of spalled oxide are responsible for most (generally greater than 90%) of the mobilization from austenitic stainless steels for steam exposures. Longer tests in VAPOR produced thicker oxides, which combined with the sharp corners on the VAPOR specimens, resulted in more spalled oxide being collected in VAPOR. Less spalled oxide was generated in FAST due to shorter oxidation times and the absence of sharp corners. Molybdenum and chromium show strong evidence of mobilization by volatilization processes during air exposures. We use FAST data at lower temperatures where better detection limits are obtained and VAPOR data at higher temperatures where higher contributions from spalled oxide provide measures of conservatism in mobilization rates for the CMFPs.

Modeling Transport of Tritium and Tritiated Water in Organic Coatings

G. R. Longhurst, ITER/UW/96/TE-SA-19,
October 4, 1996.

Tritium and tritiated water may be released into a confinement or containment structure during an accident at International Thermonuclear Experimental Reactor (ITER) or another fusion facility. An important capability in analyzing such an accident is the estimation of the uptake and release of tritium and tritiated water by the walls of the facility, most of which will be covered with a paint or coating of some sort. The TMAP4 code is adequate for modeling such events provided good information is available on the transport properties of the tritiated species through the coatings and the substrate materials.

This document surveys measurements that have been made on the transport properties of tritium and tritiated waster in various organic materials contemplated or used as surface protectants for concrete and other structural materials. General findings are that although there are differences in the specific behaviors of the various materials with respect to tritium uptake and release, the transport properties tend to fall generally in the same band for the materials reported on. Organic coatings can reduce the uptake of tritiated water by up to two or three orders of magnitude, but they don't appear to be capabile of completely eliminating the uptake. Indeed, there is a propensity for some coatings to acquire an inventory of their own, though the overall uptake by the coatings and the walls would be less than bare concrete. Where measured transport properties are available, they are presented here. Attention is also given to work done at the AECL Chalk River Laboratories where uptake in coated concrete specimens was measured but no transport properties can be definitevely generated.

Modeling of Hydrogen Plasma Interactions with Beryllium Surfaces

G. R. Longhurst, TER/US/97/TE/SA-1,
January 10, 1997.

In this EDF, we develop an improved mathematical model for interactions of hydrogen plasmas with beryllium surfaces that accounts for the saturation behavior. We justify use of that model by showing how it can be used to replicate a wide selection of both recent and past experimental data. It supports the argument that tritium inventories in the ITER first wall will be at least an order of magnitude less than was prevously thought.

Recent developments in understanding of the processes taking place in beryllium surfaces exposed to plasma ions have warranted a revisitation of the methods used in obtaining estimates for tritium inventory in plasma-facing components (PFCs) of machines such as ITER. Recently published experimental data from the Tritium Plasma Experiment (TPE) at Los Alamos National Laboratory and from other facilities have shown how the concentration of hydrogen atoms in beryllium surfaces saturates under ITER-like plasma conditions, making uptake

of hydrogen species almost independent of ion flux. Reviews of various results and modeling the TPE experiments using computational models such as the TMAP4 code confirm that surface layers develop high porosity with the result that implanting ions and atoms are readily returned to the plasma once saturation has been achieved. The same model with parameter adjustments to suit individual experiments was used to replicate results from other experiments performed at the INEEL and at Sandia National Laboratories, Livermore. Using the same transport parameters that fit the TPE experimental data, estimates of the inventory and permeation in ITER plasma-facing components during the basic performance phase suggest inventories may be only a few tens of grams rather than the few hundreds of grams estimated previously for those components. Permeation, likewise, is estimated to be very small over that same period, only a fraction of a curie per day.

Accounting for Tritium Breeding in Beryllium in TMAP4 Calculations

G. R. Longhurst, ITER/US/95/TE/SA-7 February 25,1997.

If beryllium is used as a plasma-facing material in ITER, and ITER develops the neutron fluxes it is designed to, the neutrons will cause the transmutation of some of the beryllium to tritium. This tritium source needs to be accounted for in calculations of tritium inventory and permeation in ITER. In this report, the results of previous calculations using the FISPACT code are scaled to ITER operating conditions, and a technique is developed for implementing such tritium production in the TMAP4 code. Calculations were performed using this approach for what are believed to be bounding conditions for trap concentration and trap energy. Trap concentration was assumed to be either 10,000 appm, representative of highly damaged beryllium, or 100 appm, thought to represent as-manufactured material. Trap energy was also varied between 0.8 eV, typical of as-manufactured material and 1.8 eV, thought to be associated with deuterium ion damage and therefore possibly associated with neutron effects.

The amount of tritium producted in the ITER first wall by neutron transmutations during the basic performance phase was found to be about 69 g. At low trap concentration and energy, a modest fraction of that was found to diffuse to the plasma with a little (0.04 g) making it through the first wall to the coolant stream. At the higher trap concentration but low trap energy, virtually all of the bred tritium was retained. Only about 0.003 g permeated to the coolant stream. At the higher 1.8-eV trap energy, the inventory of tritium includes not only the bred tritium, but the majority is tritium coming from the plasma and is located very close to the plasma-facing surface. Either assumption on trap concentration results in only negligible permeation to the coolant. Better information is needed regarding the nature of traps induced by the nuetrons

Tritium Inventory and Permeation Estimates in a Beryllium-Clad Lower Baffle for ITER

G. R. Longhurst, ITER/US/97/TE/SA-3, Rev. 02, March 11, 1997.

Computations were made using the TMAP4 code to estimate tritium inventory and retention in the lower baffle of ITER

under the assumption that it is clad with beryllium instead of tungsten. These calculations were made using the newly developed saturation theory that has been successful in modeling the outcomes of a number of experiments for which data are available. Two trap strengths were assumed in the beryllium, one with 0.8-eV traps at 500 appm, the other 1.8-eV traps at 1,000 appm. The present analysis also included effects of tritium breeding from neutronic transmutations and of erosion of the beryllium surface by plasma ions. This calculation estimates that after a total operating period of 7.8E6 seconds, the inventory in the lower baffle will be about 0.2 to 6 g of tritium, depending on the trap strength, including tritium bred by neutrons in the beryllium. The permeation through this structure is very low, about 0.13 g to virtually none over the whole operating period, again depending on trap characteristics. A key assumption is that the sputtering expected at the plasma-facing surface will be retarded by the presence of carbon and oxygen, as observed in the PISCES-B facility experiments.

Analysis of Tungsten Implantation Data and their Interpretation

G. R. Longhurst, ITER/US/95/TE/SA-12, August 18, 1997.

One of the important questions associated with ITER safety is the inventory of tritium in tungsten-clad plasma-facing components. Work done at the INEEL in 1991-92 gave what were determined then to be appropriate parameters for tritium transport in pure tungsten. Since then, analysis by Franzen et al. of European test data by Alimov and Scherzer and by Garcia-Rosales et al. led them to conclude that the diffusivity and recombination coefficient in tungsten were much lower and trapping parameters were substantially different than we had previously determined. Those assertions, if borne out, could have a significant effect on the estimates for tritium inventory and permeation in ITER. In this work, the experimental data forming the basis of the analysis by Franzen et al. were reviewed and analyzed using techniques similar to those that were applied to the earlier INEEL work. We found that the parameters obtained by Franzen et al. were generally reasonable for the material used in the experiments they analyzed, but parameters derived here using the higher (Frauenfelder) diffusivity gave better fits to the experimental data for wrought tungsten, the material we considered here. Those parameters are different than those derived for the INEEL experiments, partly because the material used by Alimov and Scherzer and by Garcia-Rosales et al. had 3% carbon and 2% oxygen impurities whereas the material used in the INEEL experiments was 99.95% pure. There was also some concern over the way reflectance was interpreted by Alimov and Scherzer. We conclude that the previous estimates we made for tritium retention and permeation in tungsten-clad ITER structures are still acceptable and are our preferred values for ITER calculations. Existence of a saturation effect was hinted at for room temperature data in these results, but there was no evidence for it at elevated temperatures.

Tritium Inventories and Permeation Rates For The ITER Breeding Blanket And Metal-Coated Plasma-Facing Components In The Extended Performance Phase

G. R. Longhurst,ITER/US/97/TE/SA-22 Rev. 1, September 24, 1997.

This report documents calculations made of tritium inventories and permeation rates for certain components of ITER during the extended performance phase (EPP). The configuration used was largely that defined in the Safety Analysis Data List, but some information regarding the design of the tritium breeding blanket was drawn from Section 1.6 of the Detailed Design Document. These calculations include the implantation of tritium and deuterium from the plasma and neutronic transmutation in beryllium components. The assumption was made that the rapid cool down and heat up surrounding dormant periods at the end of each pulse allow the operating time to be simply concatenated. The main vehicle used in these calculations was the TMAP4 code. Specialized techniques were employed to accommodate erosion of the beryllium surfaces and the saturation effect, which limits the inventory and permeation in beryllium-clad surfaces. Erosion of tungsten will be insignificant because of its much lower sputter efficiency and its rapid redepositon. As part of this work, the tritium evolution data from Baldwin and Billone were analyzed, and improved estimates were made of the trapping parameters for neutron irradiated beryllium. Those parameters were used for beryllium components in this work. Parameters used for tungsten were the same as used in previous analyses for the basic performance phase (BPP) (ITER/US/96/TE/SA-9 Rev. 02).

Results indicate that the total inventory at the end of the EPP will be 823 g, most of it (747 g) residing in the beryllium neutron multiplier blocks in the breeding blanket, 24.5 g in the first wall, and the balance in the baffles and divertor structures. Average permeation to the pressurized water coolant streams will be approximately 0.018 g/day, mostly through the lower baffle. The beryllium neutron multiplier blocks will release about 0.16 g/day on average to the He/H_2 purge gas stream. The implication is that inventory and permeation in these structures will be higher than in the BPP but still well within design guidelines.

RISK ASSESSMENT

Potential Vacuum Hazard to Maintenance Workers and Proposed Solutions for a Cryostat Air Ingress Accident in an ITER Maintenance Tunnel

L. C. Cadwallader and C. S. Miller, ITER/US/97/EN/SA-04, September 3, 1997.

This engineering design file presents a brief analysis of some potential safety hazards that could arise in the event of a breach in the bellows or weld of a maintenance tunnel in the International Thermonuclear Experimental Reactor (ITER) during a maintenance session, and some potential solutions for these hazards. Personnel safety around high vacuum systems is a concern because fatalities have occurred near breached vacuum systems. This analysis includes a review of energy sources that might create a hazard and a discussion of techniques that could be used to increase worker safety.

Preliminary Cryoplant FMEA

L. C. Cadwallader, ITER/US/97/EN/SA-05, September 19, 1997.

This failure modes and effects analysis (FMEA) of the International Thermonuclear Experimental Reactor (ITER) cryogenic liquid production plant, or cryoplant, is performed to support accident analysis in the Non-site Specific Safety Report (NSSR-2). When possible, individual components have been analyzed. Otherwise, generic components have been assumed to exist in the design based on what is used in other cryogenic facilities, with more generic failure modes instead of component-specific failure modes. The ITER Design Description Document (DDD) for the cryoplant was used to obtain the cryoplant design. Unfortunately, the controls for the cryoplant have not been designed at this time. Therefore, controls will not be included in this FMEA. In general, there is little description of the safety aspects of the cryoplant. If needed, then recommended safety design practices from industry and from best practices will be assumed for the ITER design in this analysis. The failure modes of specific components are discussed.

Preliminary Cryodistribution FMEA

L. C. Cadwallader, ITER/US/97/EN/SA-06, September 19, 1997.

This failure modes and effects analysis (FMEA) of the International Thermonuclear Experimental Reactor (ITER) cryogenic liquid distribution system is performed to support accident analysis in the Non-site Specific Safety Report (NSSR-2). When possible, individual components have been analyzed. Otherwise, generic components have been assumed to exist in the design based on what is used in other cryogenic facilities, with more generic failure modes instead of component-specific failure modes. The ITER Detailed Design Description (DDD) for the cryodistribution system was used to obtain design information. Unfortunately, the controls for this system have not been designed at this time. Therefore, controls will not be included in this FMEA. There is a very small description of the safety aspects of the cryodistribution system in the DDD. If

needed, recommended safety design practices from industry and from best practices will be assumed for the ITER design in this analysis. Another issue is the demarcation between the distribution system and the cryoplant system. In general, the distribution system will cover cryogen routing (piping, pumps, valves) and the accumulator tanks, not the compressors or other equipment normally regarded as production plant equipment. As the design matures, this assumption can be revisited. The failure modes of specific components are discussed.

Preliminary Master Logic Diagram for ITER Operation

L. C. Cadwallader, ITER/US/97/EN/SA-07, September 4, 1997.

This engineering design file (EDF) describes the work performed to develop a master logic diagram (MLD) for the operations phase of the International Thermonuclear Experimental Reactor (ITER). The MLD is a tool used in risk assessment to identify the broad set of potential initiating events that can present a hazard to the public, such as offsite release of radioactive materials or toxic chemicals. This MLD is complementary to the failure modes and effects analyses (FMEAs) that are being performed for ITER's major plant systems in the engineering evaluation of the facility. While the FMEAs are a bottom-up or 'component level' approach, the MLD is a top-down or 'facility level' approach to identify the broad spectrum of potential events. Strengths of the MLD are that it depicts completeness in the accident initiator process, provides an independent method for identification, and can also identify potential system interactions. MLDs have been used successfully as a hazard analysis tool.

An Enclosure Thermal Radiation Heat Transport Model for the MELCOR Code

B. J. Merrill, ITER/US/97/TE/SA-04, January 31, 1997.

First-wall surface temperatures during accident conditions in ITER play a primary role in determining the amount of hydrogen produced though the oxidation reaction of beryllium with steam. This temperature depends on radiant heat transfer to cooler components within the vacuum vessel. The existing MELCOR radiation model does not allow for the direct exchange of radiant power between such components, or account for the presence of an atmosphere between these components that absorbs and re-radiates this power. This engineering design file (EDF) describes a new thermal radiation heat transport capability that has been added to the MELCOR code to correct this deficiency. This model has been found to agree with a textbook example problem and to give the correct answer in the limit of a perfectly absorbing atmosphere. A variety of input options were tested, along with the restart capability, to ensure that the model is in working order. A transient calculation was performed and the trends, along with a global conservation of energy, indicates that the model is working properly. The transient behavior of this model was also benchmarked against the CONTAIN code and was found to be in excellent agreement with the CONTAIN enclosure radiation model.

These modifications were proposed in an assessment of the MELCOR code performed in 1994, and undertaken in 1997 after revising ITER Joint Central Team (JCT) Task Agreement S 81 TT 03 95-02028 FU, subtask 2, entitled System Level Transient Thermal-Chemical Codes. These revisions were made because of changes in research and development (R&D) priorities prompted by results from the Non-site Specific Safety Report-1 (NSSR-1).

MELCOR Pretest Predictions of the ICE Experiments

S. T. Polkinghorne, ITER/US/96/TE/SA-22, November 18, 1996.

Pretest predictions for eight ingress-of-coolant event (ICE) experiments have been performed with the MELCOR code. The ICE experiments are intended to simulate the blowdown of high-pressure, high-temperature water into the vacuum vessel of a nuclear fusion reactor as a result of a first-wall coolant tube rupture. The main objective of the experiments is to obtain data for validating safety analysis codes, such as MELCOR. The ICE experimental apparatus, the MELCOR input model, and the results of the pretest predictions are described in this report. Some key results from the pretest predictions are summarized below. The vacuum vessel pressure response is governed by the boiler water temperature (the 200°C experiments pressurized faster than the 100°C experiments), the vacuum vessel wall temperature (the 250 °C experiments generally pressurized faster than the 150°C experiments), and the presence of noncondensible gas (air) in the system (condensation rates were considerably higher for the 1 Pa experiments than

for the 100 kPa experiments). A sensitivity study showed that when a single control volume is used to model the vacuum vessel, the pressure response is nearly the same as when multiple control volumes are used. Potential limitations of the MELCOR model are also identified in this report.

Preliminary Post-Test Analysis of ICE Experiments using MELCOR

S. T. Polkinghorne, ITER/US/97/TE/SA-9 March 18, 1997.

Several ingress-of-coolant event (ICE) pretest calculations performed in 1996 with the MELCOR code were rerun using a modified model of the ICE experimental apparatus. The pretest calculations under-predicted vacuum vessel pressurization rates because boiling on the target plate was not accounted for. Therefore, the MELCOR ICE model was renodalized so that heat transfer between the liquid jet and the target plate is now simulated. Also, in keeping with the experiments, the isolation valve between the vacuum vessel and the blowdown tank was not allowed to open. In the pretest calculations, the isolation valve automatically opened when the pressure in the vacuum vessel reached 190 kPa. The calculated and measured vacuum vessel pressure transients are compared in this EDF. (A more detailed post-test analysis of the ICE experiments was not performed due to time constraints.) The revised calculations were found to be in much better agreement with the experimental data than the pretest calculations.

Pretest Predictions of ICE and LOVA Experiments using MELCOR

S. T. Polkinghorne, ITER/US/97/TE/SA-10, March 24, 1997.

Pretest predictions for several ingress-of-coolant event (ICE) and loss-of-vacuum accident (LOVA) experiments were performed with the MELCOR code. The ICE experiments are intended to simulate the blowdown of high-pressure, high-temperature water into the vacuum vessel (VV) of a nuclear fusion reactor as a result of a first-wall coolant tube rupture. The LOVA experiments are intended to simulate a breach of the vacuum boundary, resulting in air ingress into the VV. The main objective of the ICE and LOVA experiments is to obtain data for validating safety analysis codes, such as MELCOR. Some key results from the ICE and LOVA calculations are summarized as follows:

ICE: The isolation valve between the VV and the blowdown tank was only predicted to open for the first ICE experiment (200°C water, 250°C VV wall). The isolation valve automatically opened at 2.7 s when the VV pressure reached 190 kPa. For the second and third ICE experiments (200°C water, 100°C wall; and 120°C water, 50°C wall), the pressure rise was limited by condensation on the VV walls. The fourth ICE experiment was the same as the first except that the isolation valve was not opened. The VV pressure was 836 kPa and still increasing in the fourth experiment when the calculation was stopped at 200 s. Because the isolation valve was not predicted to open for experiments 2 and 3, it was not necessary to simulate experiments 5 and 6 (which are the same as experiments 2 and 3 except that the isolation valve is not allowed to open).

LOVA: The first four LOVA experiments have already been performed. These experiments were conducted at atmospheric pressure with the VV initially filled with He at room-temperature or 100°C. Data from the first experiment were used to calibrate the MELCOR LOVA model. The VV mass increased more for breach S1 (on the side of the VV) than for breach T1 (on top the VV). The VV mass also increased more for the room-temperature experiments than for the 100°C experiments. The MELCOR results for these experiments were in reasonable agreement with the data. Four pretest calculations simulating air ingress into an evacuated VV were also performed. In each case, the VV rapidly filled with air when the breach opened. A buoyancy-driven, countercurrent flow was then established (for the 100°C experiments in particular) with cool air flowing into the VV and warm air flowing out. Air exchange rates were greater for breach S1 than for breach T1.

Documentation of New MELCOR Flow Boiling, EOS, and Diffusion Coefficient Subroutines

R. L. Moore, ITER/US/97/TE/SA-6, May 12, 1997.

The MELCOR code is used at the INEEL to help evaluate the safety of the International Thermonuclear Experimental Reactor (ITER). To accomplish this task, new subroutines were added to MELCOR This EDF documents the five new subroutines which were added to MELCOR. The five subroutines added to MELCOR are HSBOIL2, EOSAIR, PSATAIR, DABMIXS, and DIFH2O. Subroutine HSBOIL2 is used to calculate heat transfer coefficients for the various modes of heat transfer encounter during flow boiling. Subroutine EOSAIR is used to determine air properties. Subroutine PSATIR is used to determine the saturation pressure for a given temperature along the bubble line of air. The final two subroutines, DABMIX and DIFH20, were added to determine the diffusion coefficients for one gas in a mixture of gases.

Results from all the added subroutines have been compared to either data when available (EOSAIR, PSATAIR, DABMIX, and DIFH2O), or have been benchmarked (HSBOIL2) against the RELAP5 code. In all cases the agreement between the subroutine generated results and the data or RELAP5 code results have been good. Since subroutines DABMIX and DIFH2O both calculate the same information it is recommended that subroutine DABMIX be used exclusively for all diffusion coefficient calculation involving one gas in a mixture of gases.